AD_____

Award Number: DAMD17-01-1-0277

TITLE: Recombinational Repair Genes and Breast Cancer Risk

PRINCIPAL INVESTIGATOR: Naoko Shima, Ph.D.

CONTRACTING ORGANIZATION: The Jackson Laboratory
Bar Harbor, Maine 04609-1500

REPORT DATE: July 2003

TYPE OF REPORT: Annual Summary

PREPARED FOR: U.S. Army Medical Research and Materiel Command
Fort Detrick, Maryland 21702-5012

DISTRIBUTION STATEMENT: Approved for Public Release;
Distribution Unlimited

The views, opinions and/or findings contained in this report are those of the author(s) and should not be construed as an official Department of the Army position, policy or decision unless so designated by other documentation.

# REPORT DOCUMENTATION PAGE

Form Approved
OMB No. 074-0188



| 1. AGENCY USE ONLY (Leave blank) | 2. REPORT DATE | 3. REPORT TYPE AND DATES COVERED |
|---|---|---|
| | July 2003 | Annual Summary (1 Jul 2002 - 30 Jun 2003) |

**4. TITLE AND SUBTITLE**
Recombinational Repair Genes and Breast Cancer Risk

**5. FUNDING NUMBERS**
DAMD17-01-1-0277

**6. AUTHOR(S)**
Naoko Shima, Ph.D.

**7. PERFORMING ORGANIZATION NAME(S) AND ADDRESS(ES)**
The Jackson Laboratory
Bar Harbor, Maine 04609-1500

*E-Mail:* nshima@jax.org

**8. PERFORMING ORGANIZATION REPORT NUMBER**

**9. SPONSORING / MONITORING AGENCY NAME(S) AND ADDRESS(ES)**
U.S. Army Medical Research and Materiel Command
Fort Detrick, Maryland 21702-5012

**10. SPONSORING / MONITORING AGENCY REPORT NUMBER**

**11. SUPPLEMENTARY NOTES**

**12a. DISTRIBUTION / AVAILABILITY STATEMENT**
Approved for Public Release; Distribution Unlimited

**12b. DISTRIBUTION CODE**

**13. ABSTRACT (Maximum 200 Words)**

To seek new double strand break (DSB) repair genes that may also influence breast cancer risk, I have developed a high-throughput screen for chromosomes instability mutants in mice. This screen has successfully yielded a recessive mutation *chaos1* (chromosome aberration occurring spontaneously 1), conferring elevated levels of spontaneous and radiation-induced micronuclei in erythrocytes.

*chaos1* was genetically mapped to a 1.3 Mb interval on Chromosome 16 that contains *Polq*, encoding DNA polymerase θ potentially involved in DNA inter-strand cross-link repair. Sequence analysis rvealed the presence of a mutant allele of *Polq* in *chaos1/chaos1* mice. A *Polq* null allele has been created by gene-targeting, and its failure to complement *chaos1* demonstrates that *chaos1* is a mutant allele of *Polq*. Interestingly, genetic interaction between *chaos1* and *Atm* (ataxia telangiectasia mutated) was observed. ATM has a central role in DSB repair, presumably influencing breast cnacer susceptibility.

We have recently identified a semi-dominant mutation *Chaos3* that was mapped to a distinct 1.3 Mb interval on Chromosome 16. We discovered a missense mutation in a candidate gene, *Mcmd4* (minichromosome maintenance deficient 4), which is essential for DNA replication licensing in all eukaryotes.

Effects of identified mutation on carcinogenesis will be investigated.

**14. SUBJECT TERMS**
No Subject Terms Provided.

**15. NUMBER OF PAGES**
31

**16. PRICE CODE**

| 17. SECURITY CLASSIFICATION OF REPORT | 18. SECURITY CLASSIFICATION OF THIS PAGE | 19. SECURITY CLASSIFICATION OF ABSTRACT | 20. LIMITATION OF ABSTRACT |
|---|---|---|---|
| Unclassified | Unclassified | Unclassified | Unlimited |

## Table of Contents

## Introduction

It was hypothesized in my proposal that DNA double strand break (DSB) repair could be one of the most important factors in breast tumor suppression, considering functions of BRCA1 and BRCA2 in DSB repair by homologous recombination (1). In addition, elevated radiosensitivity of lymphocytes from unselected breast cancer patients has been reported (2), implicating that individual difference in DSB repair may contribute to breast cancer susceptibility. DSB repair in mammals is not well understood, so there might be some unidentified genes which may influence breast cancer risk. I have chosen forward genetics approaches such as phenotype-driven mutagenesis to identify such new genes and to investigate their biological roles in the context of a whole organism.

## Body

### Task1 Screen for dominant mutants in recombinational repair using embryonic stem (ES) cells

### Task2 Use of ES cell lines bearing different deletions to screen for recessive mutants

In Task1 and 2, ES cell mutagenesis and its combination with deletion complexes in chromosomes were proposed as one of the screen methods. However, we are still developing this technology. More importantly, the experiments described in Task3 went extremely well, and I decided to focus on them.

### Task3 Screen for radiation-sensitive mutants in whole animals using a micronucleus test

#### 3.1 Recent achievements on the micronucleus screen

In my previous report, I described successful adaptation of a flow cytometric micronucleus assay (3) to screen mouse DSB repair mutants. The micronucleus assay has been used for quantitative analysis of *in vivo* chromosome damage (4, 5). Micronuclei can arise from acentric chromosome fragments or whole chromosomes that have not been incorporated in the main nuclei at cell division (6). For the enumeration of micronuclei, erythrocytes are particularly suitable, because they expel their nuclei, but not micronuclei, after their last mitotic division.

Here I briefly describe the flow cytometric assay (see Fig. 1). Micronucleated erythrocytes are stained with propidium iodide (PI) and a monoclonal antibody against the CD71 defined antigen (7) is used to divide erythrocytes into two populations. Normochromatic erythrocytes (NCEs) are low in CD71-FITC staining and micronucleated (MN)-NCEs comprise approximately 0.2-0.3% of total NCEs in wild-type mice. CD71-positive reticulocytes (RETs) account for only a few percent of total peripheral erythrocytes and MN-RETs are the rarest events (Fig. 1*a*). To facilitate the formation of micronuclei, mice can be exposed to 0.7 Gy γ-rays from a $^{137}Cs$ source. The frequency of reticulocytes with

micronuclei (MN-RETs) increased from 0.29% to 2.6% at 48 hr after γ-irradiation (Fig. 1b). Induced micronuclei would be observed in RETs, because micronucleus formation requires a mitosis and RETs in the peripheral blood are products of the most recent mitotic cycle. On the other hand, because NCEs lacked nuclei at the time of irradiation, the frequency of MN-NCEs remained relatively constant before and after irradiation; these micronuclei are of spontaneous origin. Therefore, both spontaneous and radiation-induced micronucleus levels could be measured simultaneously in the same sample.

Since a positive correlation between spontaneous and induced micronucleus levels has been reported in a number of mouse strains (8), we find it more practical and feasible to perform screens only for spontaneously elevated micronucleus levels. Potential mutants isolated can be characterized later as to sensitivity to radiation or other agents. Mice generated in the subsequent screens were tested only for spontaneous micronucleus levels. We have recovered five potential mutants from the genome wide screen and one mutation from the Chromosome 5 region-specific mutagenesis screen. The screen results are summarized in Table 1.

### 3.2 *chaos1* is a mutant allele of *Polq*

This high-throughput screen has yielded *chaos1* (chromosome aberration occurring spontaneously 1) conferring elevated levels of spontaneous and radiation- or mitomycin C-induced micronuclei (Fig. 2). This recessive mutation was genetically mapped to a 1.3 Mb interval on Chromosome 16 that contains *Polq*, encoding DNA polymerase θ. We identified a non-conservative mutation in the ENU-derived allele, making it a strong candidate for *chaos1*. POLQ is homologous to Drosophila MUS308, which is essential for DNA inter-strand cross-link repair (9). However, functions of this novel DNA polymerase have not been investigated.

To confirm that *chaos1* is a mutant allele of *Polq*, we have generated three lines of transgenic mice with a bacterial artificial chromosome (BAC) clone RPCI24-108G13 containing wild-type *Polq*. Since *chaos1* mutation was induced in C57BL/6J (B6), and the transgenic founders were also generated using B6 mice, we mated the transgenic mice with C3HeB/FeJ (C3H) congenic *chaos1/chaos1* mice (see Fig.3 for mating scheme). *chaos1* heterozygotes were backcrossed to C3H for ten generations (N10) to generate these congenic mice. More than 99% of the genome is derived from C3H except the region nearby *chaos1*. F1 males carrying the transgene were mated with C3H congenic *chaos1/chaos1* females and their progeny were genotyped for the presence of the transgene. Two polymorphic markers on chromosome 16, one proximal and the other distal, were used to distinguish the chromosomes containing *chaos1* from wild-type B6 chromosomes and also to identify recombinants. Four *chaos1/chaos1* mice without the transgene had significantly higher micronucleus frequencies ranging 0.62-0.73%, whereas six *chaos1/chaos1* mice with the transgene from two transgenic lines (lines #6354, 6355) had normal levels of micronuclei (0.14-0.32%), indicating phenotype rescue. Nevertheless one transgenic line (line #6353) failed to correct the *chaos1* phenotype. To examine expression of the *Polq* transgene of all three lines, we, therefore, performed RT-PCR on peripheral blood RNA and sequenced cDNAs. As shown in Fig.4, wild-type "T" was observed in the two

lines (#6354 and 6355), indicating expression of the transgene. On the other hand, only mutant "C" was observed in the line 6353, indicating that the transgene is silent in this line. These transgene expression data further support the phenotype rescue by the transgene.

Since this BAC clone contains a fragment of another gene, I have also constructed a gene-targeting vector for *Polq* (Fig. 5) designed to replace a part of exon1 and exons 2-5 with *neo* to create a null allele of this gene. Two targeted mouse embryonic stem (ES) cell clones were identified and injected into blastocysts for chimera production (data not shown). One germline competent chimera was identified and was mated to a *chaos1/chaos1* female to test for non-complementation. Two males carrying both *chaos1* and *Polq* null alleles showed higher micronucleus frequency (0.65-0.7%), while one heterozygote ($Polq^{+/-}$) was phenotypically normal. These results demonstrate that *chaos1* is a mutant allele of *Polq*. The germline chimera is now being used to generate homozygotes for the null allele. Comparisons of phenotypes between *chaos1* mutants and *Polq* null mice will provide additional information on gene function.

### 3.3 Genetic interaction of *chaos1* with *Atm*

Ataxia telangiectasia is human cancer syndrome due to germline mutation in ATM (ataxia telangiectasia mutated), which has a central role in double strand break (DSB) recognition and signaling of the repair pathway (10). To characterize genetic interaction between *chaos1* and *Atm*, we crossed *chaos1/chaos1* mice with *Atm* heterozygotes carrying a null mutation ($Atm^{+/-}$). *Atm* homozygotes ($Atm^{-/-}$) are sterile. Subsequent progeny were intercrossed to obtain mice with six different genotypes as shown in Table2. The number of double mutants was much less than expected by Mendelian ratios and thus the combination of these two mutations is partially lethal (Table 2). We can speculate that increased cell death caused by massive unrepaired DNA damage may contribute to the lethality during development. The exact timing and causes of the death will be determined. Surviving double mutants are severely growth retarded and show increased genome instability, although they have a much longer latency for thymic lymphoma than the $Atm^{-/-}$ mice (Fig. 6). The presence of extremely low numbers of thymocytes in the double mutants may partially explain this longer latency. The mechanism of this phenomenon will be investigated in detail, since it may have implications for potential treatment or cure of this human disease.

### 3.4 Future experiments on *Polq*

Recently, human POLQ has been purified as a high fidelity DNA polymerase with the ability to bypass abasic lesions (11). This is quite unique among recently discovered DNA polymerases, most of which are error-prone (12). POLQ is also unique in that it contains both a helicase and DNA polymerase domain. However, it remains to be elucidated how exactly this protein works in cross-link repair in higher eukaryotes, an area that is still poorly understood. Because cross-linking agents are used as anti-cancer drugs, this investigation of cross-link repair will be clinically relevant.

*Polq* null cell lines have been also created for the following *in vitro* studies. Efficiency of cross-link repair will be assayed by transfecting a plasmid with a reporter gene containing a cross-link in a specific site. Repair of the cross-link

allows expression of the reporter gene. It is known that cross-links are repaired by at least two different pathways: recombination dependent or independent. Experiments will be design to assess these two pathways.

POLQ will be tagged with epitopes to determine localization of POLQ within the cell using commercially available antibodies against the epitopes. Potential interactions of POLQ with recombination repair proteins, which are also involved in cross-link repair, will be examined for potential interaction with POLQ. Since purified human POLQ does not exhibit helicase activity, it has been suggested that POLQ might be cleaved into a few polypeptides after translation. Therefore N-terminal helicase and C-terminal DNA polymerase domains will be tagged with different epitopes in order to track activities of both domains.

**3.5 Identification of a semi-dominant mutation *Chaos3***

In addition to *chaos1*, we have recently identified a new mutation that also confers elevated spontaneous micronucleus frequencies and named it *Chaos3*. *Chaos3* mutant mice do not exhibit radiation sensitivity, as do *chaos1/chaos1* mice. Although *Chaos3* was isolated from the Chromosome 5 screen (see Table 1), this mutation does not map on this chromosome. Since five *Chaos3* mutants were recovered from a litter of seven, we speculated that this mutation might be dominant or semi-dominant. Because the parents of these original *Chaos3* mutants were not available for phenotype analysis, we crossed *Chaos3* mutant mice with wild-type C3H mice and phenotyped their progeny. All of the original *Chaos3* mutants were identified as heterozygotes, because about half of the progeny from each mutant were mutants. Thus, *Chaos3* is transmitted as a dominant or semi-dominant manner.

A genome scan was performed with microsatellite markers polymorphic between B6 and C3H on the mutant progeny DNA. Because they are also heterozygotes (they inherited a wild-type allele from the C3H parents) and *Chaos3* was induced in B6 genome, we sought a region heterozygous for B6/C3H in all DNA samples. Sixty meioses were examined, linking *Chao3* to a 17.9 Mb interval between *D16Mit165* and *D16Mit103* on Chromosome 16. Intercrosses between heterozygotes produced mice homozygous at this region with expected Mendelian ratios. These mice have astonishingly elevated spontaneous micronucleus frequencies up to 20 fold over wild-type mice, while the heterozygotes with only 2-3 fold increase (Fig. 7). Observing a distinct phenotype in the homozygotes, we defined *Chaos3* as a semi-dominant mutation.

**3.6 *Chaos3* fine mapping**

To increase the level of polymorphism, thereby enhancing mapping resolution, an inter-subspecific mapping cross between *Chaos3* and *Mus castaneus* (CAST/Ei) were performed. *Chaos3* heterozygotes were crossed with CAST/Ei and then F1 mice heterozygous at *Chaos3* were either intercrossed or backcrossed to CAST/Ei. Resulting 971 meioses were examined, localizing *Chaos3* on a 1.6 Mb region between *D16Mit56* and *D16Mit74*. Exploiting the mouse genomic sequences in the Celera discovery system™ (CDS), we developed new microsatellite markers polymorphic between B6 and CAST/Ei on this region. The *Chaos3* critical region now spans a 1.3 Mb interval between *D16Mit56* and a new marker *D16Jcs61* (Fig. 8). This region contains 19 genes predicted by CDS, including *Mcmd4* (minichromosome maintenance deficient 4), which is essential

for the initiation of DNA replication in all eukaryotes. *Prkdc* encoding protein kinase (DNA activated) catalytic subunit also resides in the *Chaos3* critical region. However, because *Chaos3* does not confer increased sensitivity to radiation, I did not consider it as a candidate for this mutation. Rather, I hypothesized that *Chaos3* might be involved in DSB repair during DNA replication or DNA replication itself. Therefore I prioritized *Mcmd4* as a candidate for *Chaos3*.

### 3.7 *Chaos3*, a potentially novel mutation of the MCM family

Reverse transcription-polymerase chain reaction (RT-PCR) was performed on testis RNA obtained from *Chaos3* homozygotes to yielded partial cDNAs of *Mcmd4*. There was no indication of differences in transcript size or expression levels in mutant RNA compared to that from wild-type B6 mice. Nevertheless, a single T to A base substitution was identified at the nucleotide1033 in the coding region (exon 8) of *Chaos3* homozygotes (Fig. 9), that is not present in B6 cDNA. T to A transversion agrees with mutation spectra induced by ENU, which was used as mouse germline mutagen in this screen (13). This mutation creates an amino acid change from phenylalanine to isoleucine at residue 345 (Phe345Ile), 15 amino acids downstream of the zinc finger motif. The flanking region of the zing finger has been shown to be important for DNA binding and interaction with other MCM proteins (14, 15).

The MCM family consists of six conserved proteins that are essential for the initiation of DNA replication in all eukaryotes (reviewed in 16, 17). These proteins interact with each other to form a hexameric MCM2-7 complex that plays a central role in restricting DNA synthesis to once per cell cycle. The MCM complex serves as the helicase that melts replication origins at initiation and then acts as the replicative helicase during elongation of replication forks (18). Studies on yeast and Drosophila *mcm* mutants have provided valuable data for our current understanding of MCM protein function in DNA replication. Moreover, MCM proteins have been investigated as a pre-cancer marker (19). Recently a new member of MCM family, *MCM8* was isolated as a cancer-related gene in humans (20), thereby indicating potential roles of this family in carcinogenesis. Therefore, *Chaos3* could be very useful in investigating potential roles of MCM proteins in cancer.

### 3.8 Future experiments on *Chaos3*

The following strategies will be taken to confirm *Chaos3* as a *Mcmd4* mutant. Mutant MCM4 will be over-expressed in ES cells to determine whether or not it has dominant-negative effects that may cause the semi-dominant *Chaos3* phenotypes. Alternatively, one of the wild-type alleles will be replaced with the mutant allele in ES cells by "knock-in" approach in case *Chaos3* phenotypes are due to haplo-insufficiency of *Mcmd4*. The effect of the identified mutation will be confirmed in chimeras derived from ES cells containing mutant MCM4. Moreover, the potentially abnormal association of mutant MCM4 with other MCM proteins and with chromatin will be also examined, since the identified mutation Phe345Ile may affect the zing finger functions.

It has been demonstrated that proteins involved in DNA replication are necessary for establishment of proper chromosome condensation, a critical process to ensure normal chromosome segregation at mitosis. Abnormally condensed chromosomes have been observed in Drosophila MCM mutants (21,

22). These abnormal chromosomes frequently contain indistinguishable centromeres and/or lack sister chromatid cohesion. Metaphase spreads will be analyzed in embryonic fibroblasts derived from *Chaos3* homozygotes to examine chromatin condensation and the presence of aberrant chromosomes. I will investigate how these events are related to higher spontaneous micronucleus frequencies observed in this mutant.

**Task4 Investigation of effects of meiosis-specific DMC1 on mitotic recombination**

We are still seeking a suitable system, which ensures stable expression of *Dmc1* in somatic cells.

**Key Research Accomplishments**

- It has been confirmed that *chaos1* is a mutant allele of *Polq* by transgene rescue and by complementation test with a *Polq* null allele created by gene-targeting.

- Double homozygous mutants for *chaos1* and *Atm* mostly die before birth. Surviving double mutants are severely growth retarded. However they seem to have a much longer latency for lymphoma than *Atm* single mutants. These data suggest genetic interaction between these two genes.

- A new mutation *Chaos3* has been isolated and mapped on a distinctive 1.3 Mb region on Chromosome 16. *Chaos3* mutant mice contain a missense mutation in a candidate gene *Mcmd4*, which has essential roles for DNA replication licensing.

- Five potential mutations have been also recovered and await further analysis.

**Reportable outcomes**

**Presentation**

**Shima N**, Hartford SA, Duffy T, Wilson LA, Schimenti KJ, Schimenti JC
Two chromosome instability mutants identified by mouse ENU mutagenesis screen, Gordon Research Conference, Mammalian DNA repair, January 2003, Ventura, California

**Publication**

**Shima N**, Hartford SA, Duffy T, Wilson LA, Schimenti KJ, Schimenti JC (2003)
Phenotype-based identification of mouse chromosome instability mutants, Genetics 163: 1031-1040

**Conclusions**

Isolated mutation *chaos1* has been proven as a mutant of novel DNA repair gene *Polq*, which shows genetic interaction with *Atm*, a key player in DSB repair signaling. *Polq* null mice and cell lines have been created by gene-targeting. Phenotype analyses of them will be informative on exploring *Polq* function in DNA repair.

The high throughput micronucleus screen has yielded more mutations including *Chaos3*. A candidate gene *Mcmd4* is mutated in *Chaos3* mutant mice.

*Mcmd4* is an essential gene required for DNA replication and its complete inactivation will be lethal. Therefore viable *Chaos3* mutant mice are very useful for in vivo studies. Potential roles of MCM4 in cancer will be investigated in *Chaos3* mutant mice.

Identification of *Chaos3* suggests a great potential of this phenotype-based screen to recover mutants defective in DNA replication, a fundamental cellular process. With this screen, it may be possible to identify mutations in genes in involved in diverse pathways of DNA metabolism, as long as they exhibit elevated levels of spontaneous micronuclei.

**References**


1. A. R. Venkitaraman, *Cell* **108**, 171-82. (2002).
2. D. Scott, J. B. Barber, A. R. Spreadborough, W. Burrill, S. A. Roberts, *Int J Radiat Biol* **75**, 1-10. (1999).
3. S. D. Dertinger, D. K. Torous, K. R. Tometsko, *Mutat Res* **371**, 283-92. (1996).
4. J. A. Heddle, *Mutat Res* **18**, 187-90. (1973).
5. T. Morita, et al., *Mutat Res* **389**, 3-122. (1997).
6. M. Nusse, B. M. Miller, S. Viaggi, J. Grawe, *Mutagenesis* **11**, 405-13. (1996).
7. S. Serke, D. Huhn, *Br J Haematol* **81**, 432-9. (1992).
8. M. F. Salamone, K. H. Mavournin, *Environ Mol Mutagen* **23**, 239-73 (1994).
9. P. V. Harris, et al., *Mol Cell Biol* **16**, 5764-71. (1996).
10. M. S. Meyn, *Clin Genet* **55**, 289-304. (1999).
11. G. Maga, I. Shevelev, K. Ramadan, S. Spadari, U. Hubscher, *J Mol Biol* **319**, 359-69. (2002).
12. M. F. Goodman, B. Tippin, *Nat Rev Mol Cell Biol* **1**, 101-9. (2000).
13. M. J. Justice, J. K. Noveroske, J. S. Weber, B. Zheng, A. Bradley, *Hum Mol Genet* **8**, 1955-63 (1999).
14. G. S. Yan H, Tye BK., *Genes Dev* **5**, 944-57 (1991).
15. I. Y. You Z, Masai H, Hanaoka F., *J Biol Chem* **277**, 42471-9 (2002).
16. T. BK., *Annu Rev Biochem* **68**, 649-86 (1999).
17. T. B. Lei M, *J Cell Sci* **114**, 1447-54 (2001).
18. T. J. Labib K, Diffley JF, *Science* **288**, 1643-7 (2000).
19. O. I. Ishimi Y, Kato C, Kwon HJ, Kimura H, Yamada K, Song SY, *Eur J Biochem* **270**, 1089-101 (2003).
20. K. Y. Johnson EM, Daniel DC, *Nucleic Acids Res* **31**, 15-25 (2003).
21. B. M. Pflumm MF, *Development* **128**, 1697-707 (2001).
22. T. B. Christensen TW, *Mol Biol Cell* **14**, 2206-15 (2003).

Table1 Summary of recent data on the micronucleus screen

| Type of Screen | No. of Mice Screened | No. of Families Screened | No. of Potential Mutants |
|---|---|---|---|
| Genome-wide* | 1661 | 154 | 5 |
| Chromosome 5* | 450 | 450 | 1** |

*Detailed description of these screens was given in my previous report.
**This is a confirmed mutation *Chaos3* (see the text), but is not on chromosome 5.

Table 2 Results of intercrosses between *Atm*$^{+/-}$;*chaos1*/+ and *Atm*$^{+/-}$;*chaos1*/*chaos1*

| Genotype *Atm* / *chaos1* | +/+ +/- | +/+ -/- | +/- +/- | +/- -/- | -/- +/- | -/- -/- | Total |
|---|---|---|---|---|---|---|---|
| No. of mice | 44 | 38 | 98 | 70 | 29 | 3 | 282 |
| Expected | 30.25 | 30.25 | 70.5 | 70.25 | 30.25 | 30.25 | $p<0.001$* |

*By $\chi 2$ test

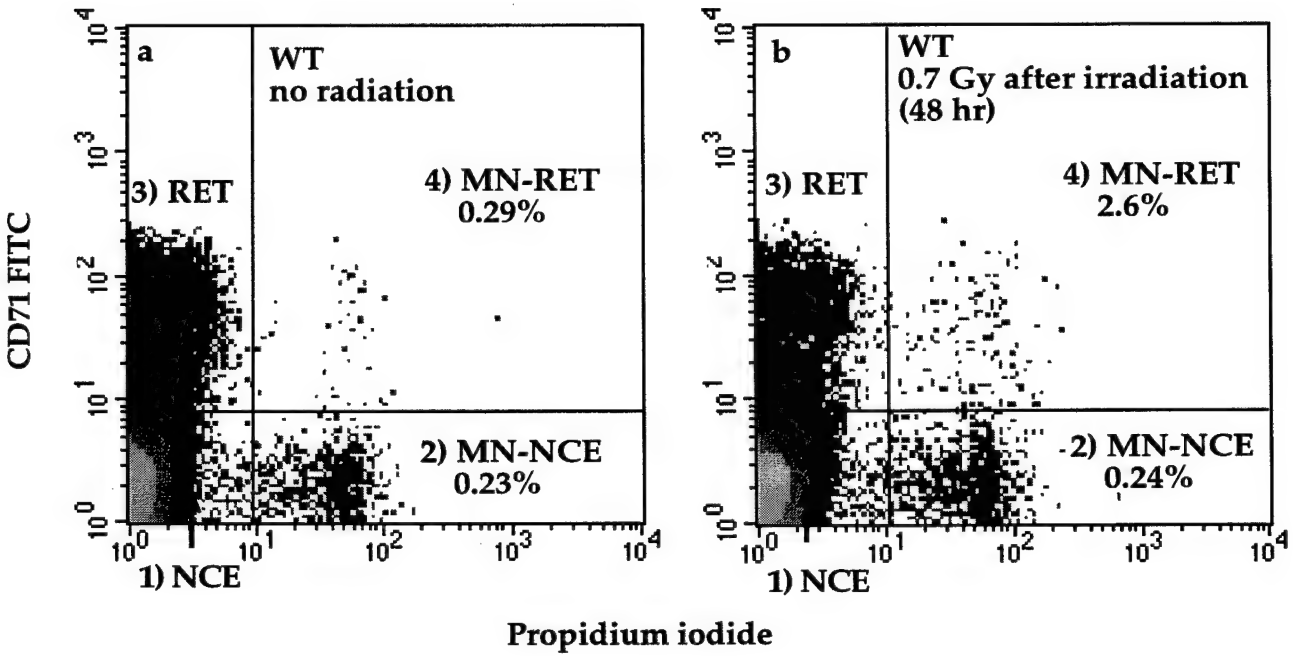


Fig.1 Representative plots of the flow-cytometric micronucleus assay. Peripheral blood from a wild-type animal before (a) and 48 hr after irradiation (b) was analyzed. CD71-positive RETs (populations 3 and 4) are separated from CD71-negative NCEs (populations 1 and 2) to enumerate radiation-induced micronuclei. MN-NCEs and MN-RETs are stained with propidium iodide and shown as populations 2 and 4, respectively. At least 50,000 NCEs and 10,000 RETs are analyzed.

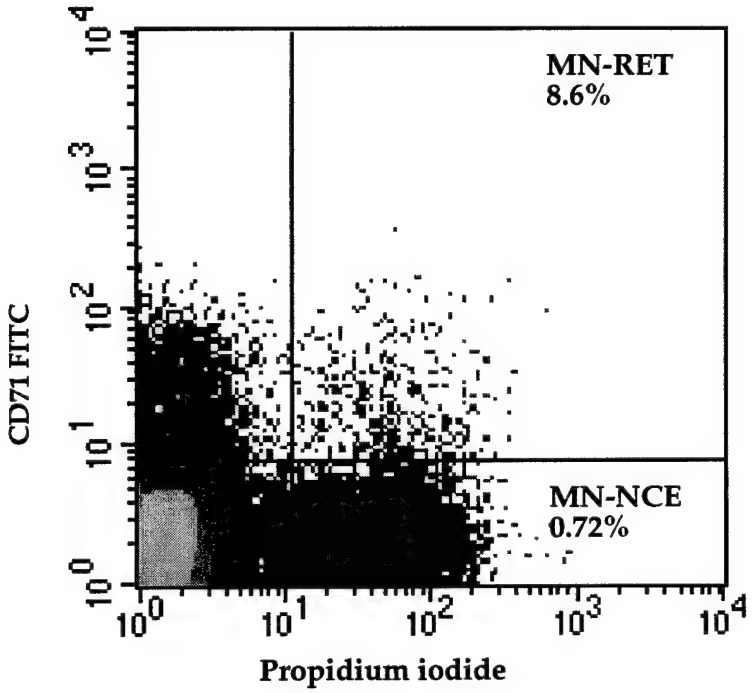


Fig. 2 Elevated spontaneous and radiation-induced micronucleus frequencies of *chaos1/chaos1* mouse. Two million erythrocytes had to be analyzed to collect 5,000 RETs, because of extremely low number of RETs after irradiation.

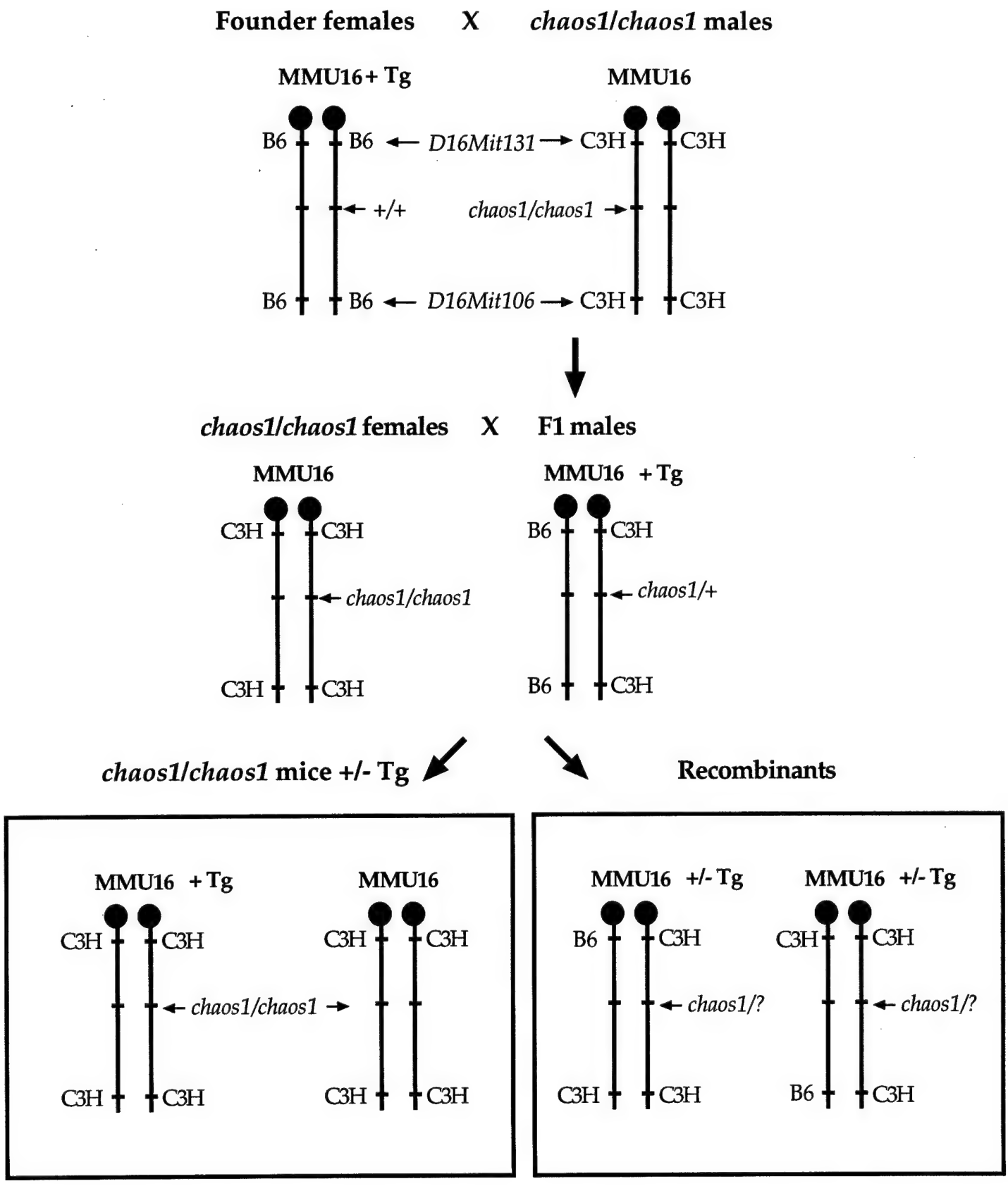


Fig.3 Mating scheme for the BAC rescue experiment. The transgenic founder females (B6) were mated with C3H congenic *chaos1/chaos1* males. F1 males carrying the transgene (Tg) were identified and mated with C3H congenic *chaos1/chaos1* females. Subsequent progeny were genotyped for *chaos1*, using proximal *D16Mit131* and distal *D16Mit106* markers polymorphic between B6 and C3H, and for the presence of the transgene. All progeny were phenotyped and all mice carrying the transgene (from line #6354 or#6355) were identifed as wild-type, including the recombinants in which genotype for *chaos1* mutation is unknown.

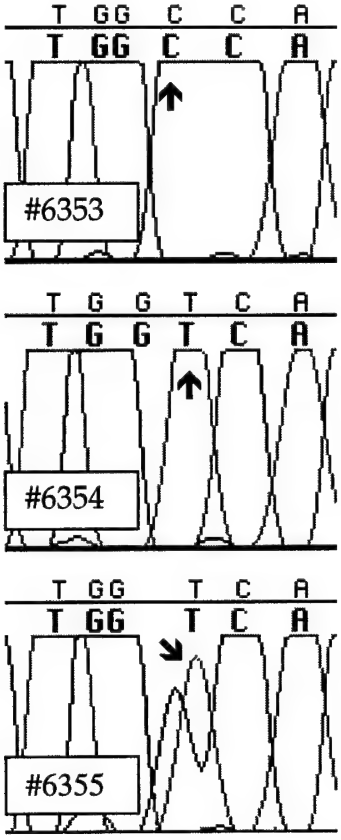


Fig. 4 Expression data on the *Polq* transgene. Line #6353 shows only mutant **C**, indicating no expression of the wild-type *Polq* transgene. In the other lines #6354 and #6355, wild-type T can be observed. Particularly in the line #6354, the transgene seems to be highly expressed, because of the absence of mutant **C** in the amplified cDNA, whereas the line #6355 has both of wild-type **T** and mutant **C** peaks.

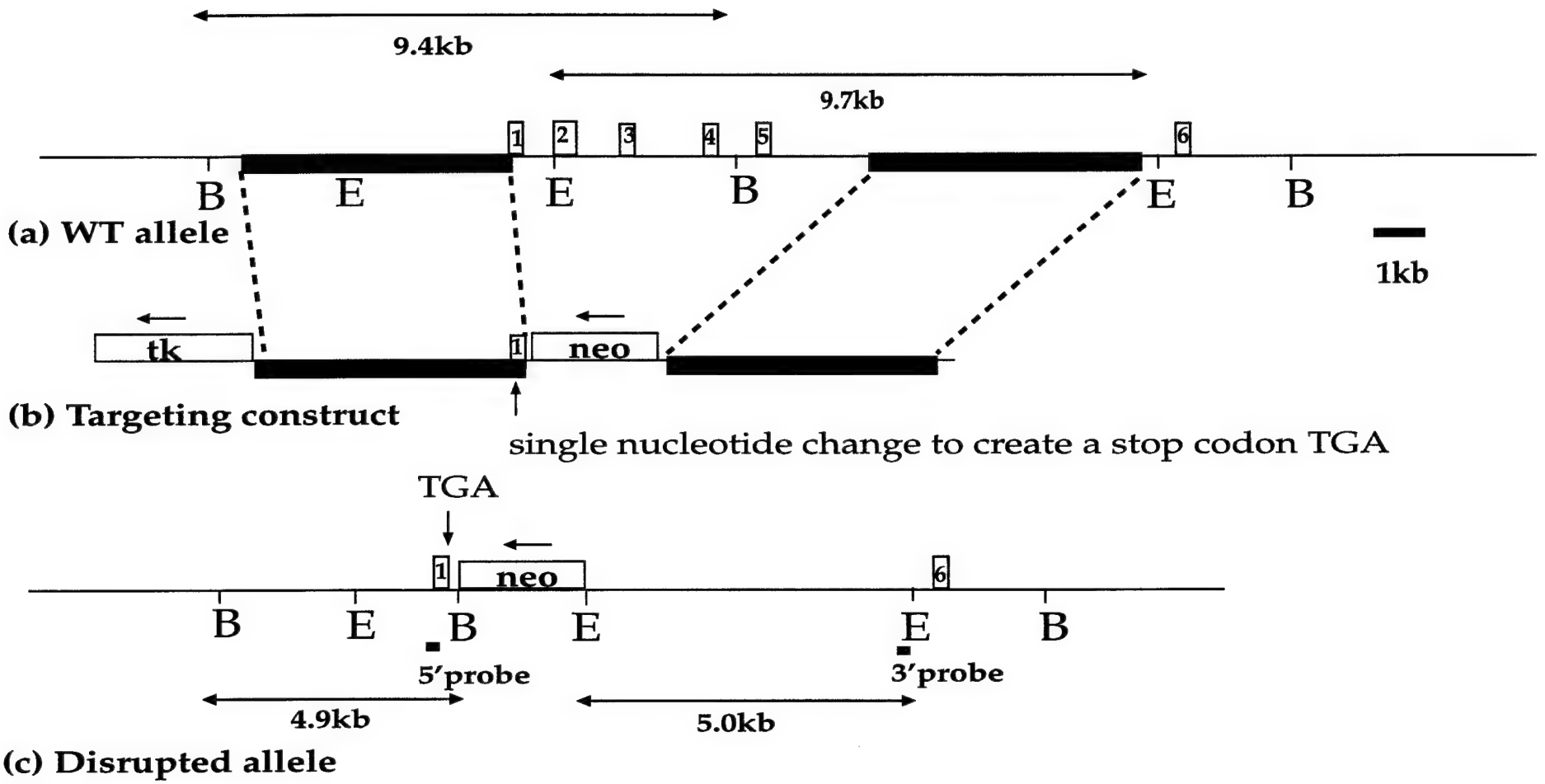


Fig.5 *Polq* gene targeting strategy. (a) Schematic representation of part of the genomic *Polq* locus. The first six exons are indicated as boxes with numbers. Location of selected restriction sites are shown. Filled rectangles represent genomic sequences used in the targeting construct (b). The positions of the selectable marker genes tk and neo are also indicated. In disrupted allele(c), part of exon 1 and exons 2-5 are replaced with neo. To ensure creation of a null allele, a stop codon (TGA) is introduced right after the start codon in exon 1.

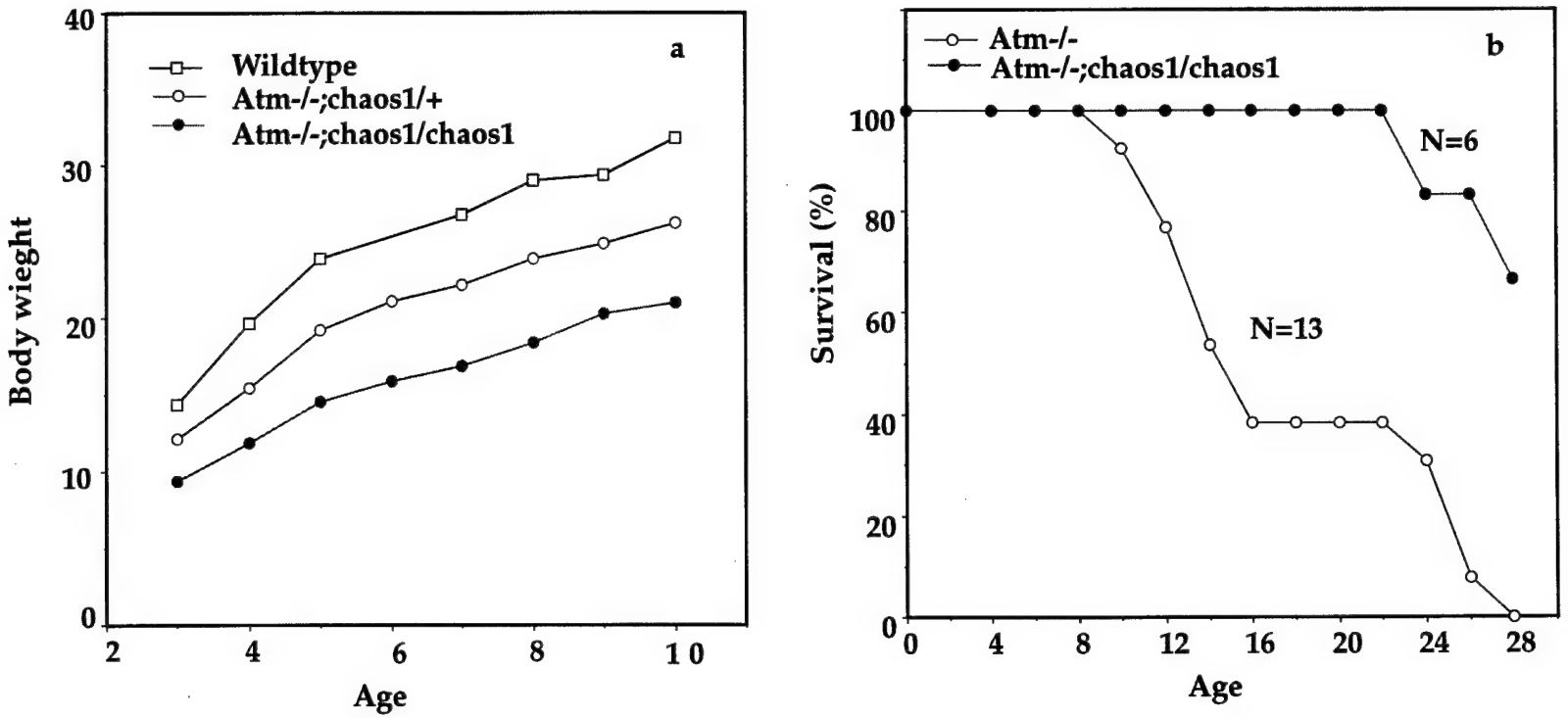


Fig. 6 Genetic interaction of *chaos1* with *Atm*. (a) Double homozygous mutants for *chaos1* and *Atm* are severely growth retarded. *Atm* single mutants are 10-20% smaller than wild-type mice and the double mutants are further smaller, approximately 40% smaller than wild-type. (b) The double mutants seem to have a longer latency for thymic lymphoma than *Atm* single mutants, since they survive significantly longer.

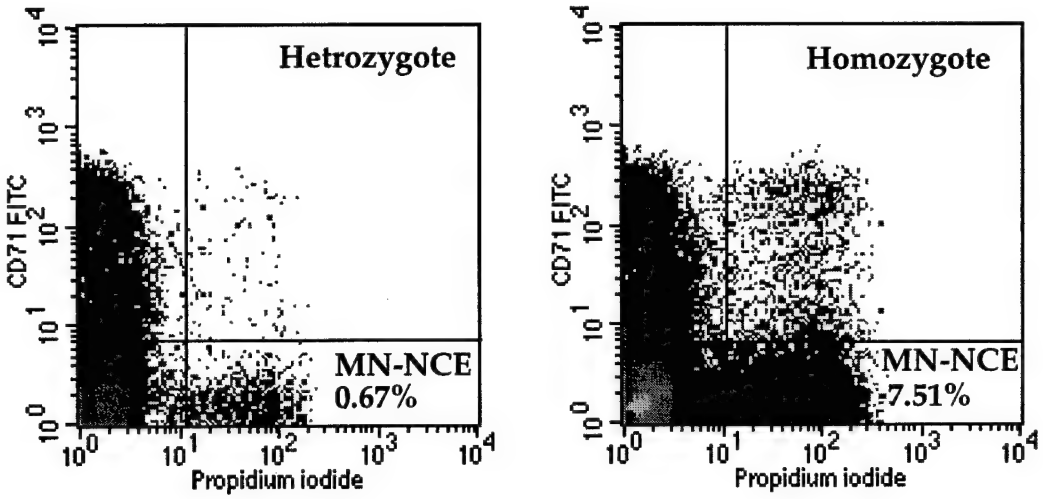


Fig. 7 *Chaos3* phenotypes. Spontaneous micronucleus frequencies were determined after collecting 20,000 NCEs. While *Chaos3* heterozygotes have 2-3 fold increase over wild-type (see Fig. 1 for wild-type) in spontaneous micronucleus formation, *Chaos3* homozygotes show 20 fold increase.

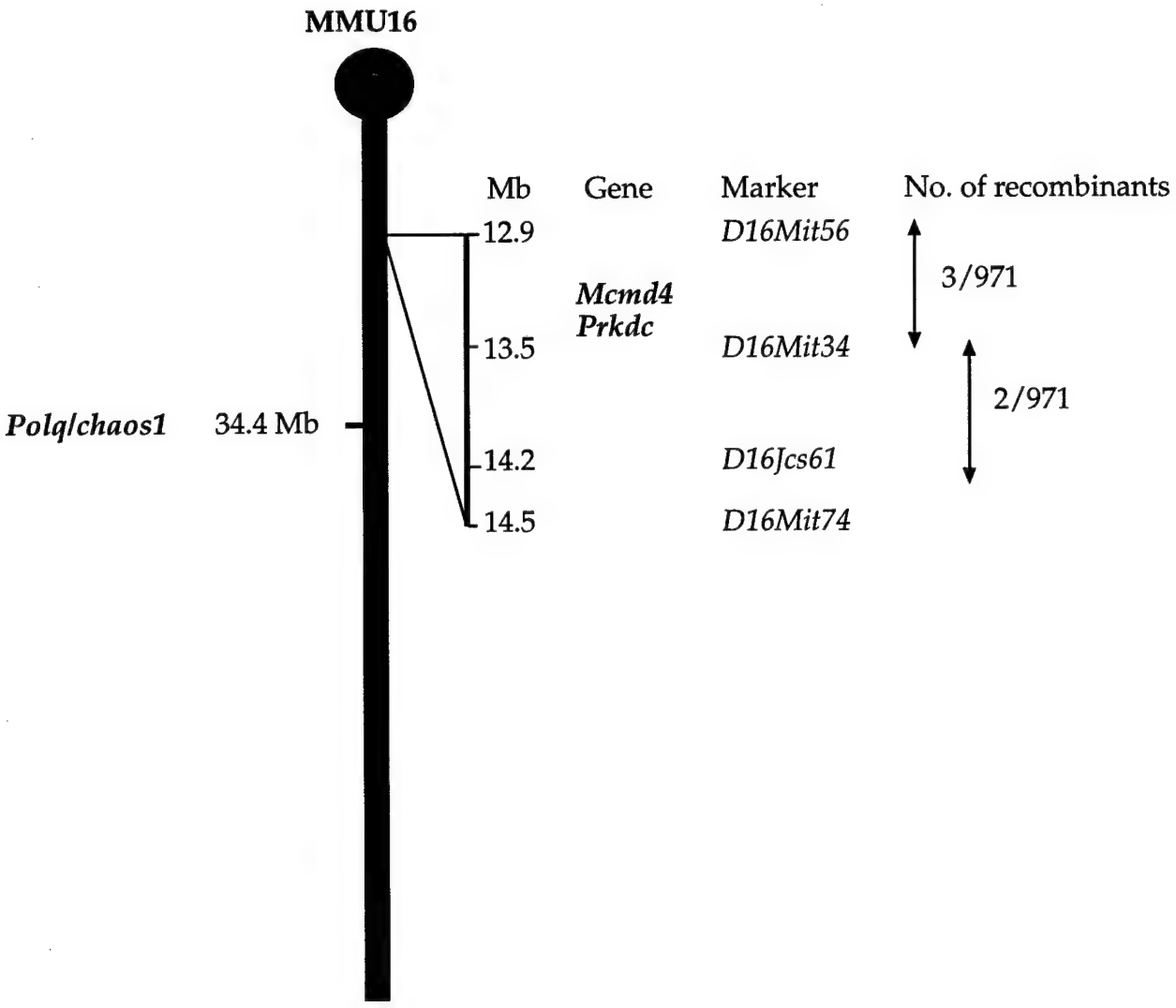


Fig. 8 The *Chaos3* critical region. Physical location of genes and microsatellite markers are shown, using data from the Celera Discovery System (CDS). *D16Jcs61* marker, which is polymorphic between B6 and CAST/Ei, was designed for this study. Data from the inter-subspecific mapping crosses between *Chaos3* and CAST/Ei are shown, which were used to determine the *Chaos3* critical region. There are 19 genes predicted by the CDS in this region. Among them, a strong candidate gene *Mcmd4* and *Prkdc* are shown here. Location of *Polq/chaos1* is also shown.

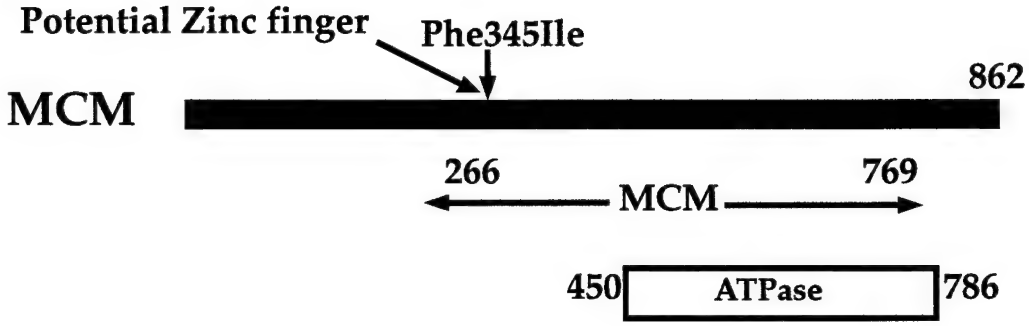


Fig.9 Phe345Ile mutation nearby the zing finger motif found in *Chaos3* mutant mice. MCM4 protein contains 862 amino acids. Conserved domains such as MCM and ATPase are indicated with corresponding amino acid numbers. Identified mutation Phe345Ile is located in a position carboxyl to the zing finger motif, which has important roles in DNA binding and interaction with other MCM members.

Appendices
Shima, Naoko

# Phenotype-Based Identification of Mouse Chromosome Instability Mutants

**Naoko Shima, Suzanne A. Hartford, Ted Duffy, Lawriston A. Wilson, Kerry J. Schimenti and John C. Schimenti[1]**

*The Jackson Laboratory, Bar Harbor, Maine 04609*

Manuscript received September 13, 2002
Accepted for publication November 20, 2002

ABSTRACT

There is increasing evidence that defects in DNA double-strand-break (DSB) repair can cause chromosome instability, which may result in cancer. To identify novel DSB repair genes in mice, we performed a phenotype-driven mutagenesis screen for chromosome instability mutants using a flow cytometric peripheral blood micronucleus assay. Micronucleus levels were used as a quantitative indicator of chromosome damage *in vivo*. Among offspring derived from males mutagenized with the germline mutagen *N*-ethyl-*N*-nitrosourea (ENU), we identified a recessive mutation conferring elevated levels of spontaneous and radiation- or mitomycin C-induced micronuclei. This mutation, named *chaos1* (*ch*romosome *a*berration *o*ccurring *s*pontaneously *1*), was genetically mapped to a 1.3-Mb interval on chromosome 16 containing *Polq*, encoding DNA polymerase θ. We identified a nonconservative mutation in the ENU-derived allele, making it a strong candidate for *chaos1*. POLQ is homologous to Drosophila MUS308, which is essential for normal DNA interstrand crosslink repair and is unique in that it contains both a helicase and a DNA polymerase domain. While cancer susceptibility of *chaos1* mutant mice is still under investigation, these data provide a practical paradigm for using a forward genetic approach to discover new potential cancer susceptibility genes using the surrogate biomarker of chromosome instability as a screen.

CHROMOSOME instability is a hallmark of cancer cells. It may arise from defects in chromosome metabolism, including DNA double-strand-break (DSB) repair. DSBs can lead to chromosome aberrations and to mitotic recombination, either of which can result in loss of heterozygosity. As seen in individuals with certain cancer syndromes, DSB repair defects may cause chromosome instability, increasing cancer risk. For example, ataxia telangiectasia and the Nijmegen breakage syndrome (Digweed *et al.* 1999; Meyn 1999) are attributed to germline mutations in genes regulating DSB repair signaling. Werner, Bloom, and Rothmund-Thomson syndromes (van Brabant *et al.* 2000) are all caused by mutations in RecQ-like genes, which are thought to be involved in repair of DSBs by homologous recombination (HR). Furthermore, the breast cancer susceptibility genes *BRCA1* and *BRCA2* also function in DSB repair, particularly in the regulation of HR (Venkitaraman 2002). Inactivation of these genes also causes genomic instability (Shen *et al.* 1998; Tutt *et al.* 1999; Kraakman-van der Zwet *et al.* 2002). In sum, DSB repair appears to have an important role in genome maintenance and tumor suppression. To achieve a full understanding of DSB repair and its association with cancer, it is necessary to identify all the genes involved.

Many mammalian genes involved in DSB repair, particularly by HR, have been identified on the basis of homology to those of the yeast *Saccharomyces cerevisiae*, indicating their conserved role in genome maintenance (Thacker 1999). However, it is likely that additional mammalian DSB repair genes do not exist in yeast. For example, there are no yeast homologs of *BRCA1*, *BRCA2*, or *PRKDC* (protein kinase, DNA-activated, catalytic polypeptide). Furthermore, mammals have a larger RAD51 family consisting of seven members with nonredundant function (Thompson and Schild 2001; van Gent *et al.* 2001). Most notably, yeast and mammalian cells have clear differences in the way they repair DSBs. There are two major pathways in DSB repair in mammalian cells, HR and nonhomologous end joining (NHEJ; Karran 2000; Khanna and Jackson 2001; van Gent *et al.* 2001). NHEJ is used heavily in mammalian cells, whereas in yeast, DSBs are repaired almost exclusively by HR (Thompson and Schild 1999). The NHEJ pathway, which is also involved in V(D)J recombination, joins broken chromosomal ends with little homology and thus is error prone. In the HR repair pathway, a sister chromatid or homologous chromosome is used as a repair template, resulting in higher fidelity. This pathway may be more important during development, since inactivation of most of HR genes results in early embryonic lethality (Thompson and Schild 2001). It has been suggested that activities of the two DSB repair pathways may be regulated during the cell cycle in mammals (Hendrickson 1997; Thompson and Schild 1999, 2001).

Sequence data from this article have been deposited with the EMBL/GenBank Data Libraries under accession nos. AY074936, AY147862, AY147863, and AY147864.

[1]*Corresponding author:* The Jackson Laboratory, 600 Main St., Bar Harbor, ME 04609. E-mail: jcs@jax.org

DSB repair mutants have been traditionally isolated on the basis of radiation hypersensitivity in yeast and rodent cell lines (THOMPSON *et al.* 1982; JONES *et al.* 1987, 1988; FRIEDBERG *et al.* 1995). At least 11 complementation groups of X-ray-sensitive rodent cell line mutation have been identified (ZDZIENICKA 1999). Eventually, the *in vivo* consequences of mutations in some of these genes were investigated by the generation of gene-targeted mice. Since most of these mutations are recessive, it has been suggested that the mutant identification depended on aneuploidy and/or presence of hemizygous loci in these cell lines (JONES *et al.* 1988). Thus it is possible that many genes were undetectable by such screens.

Forward genetic mutation screens in mice offer several advantages for the identification of new DSB repair genes. Random *N*-ethyl-*N*-nitrosourea (ENU) mutagenesis of the mouse genome is now a well-established method to isolate both dominant and recessive mutations with high efficiency (JUSTICE *et al.* 1999; HRABE DE ANGELIS *et al.* 2000), and positional cloning of these mutations has been vastly simplified by the availability of mouse genomic sequence and various other genetic resources. If an efficient assay were available to detect chromosome instability, it could be exploited in forward genetic mutation screens to identify novel genes required for DSB repair and/or chromosome stability in mice. Moreover, potential cancer susceptibility can be addressed directly in the mutant mice.

To detect mouse DSB repair mutants, we explored the efficacy of a high-throughput micronucleus assay, which provides a quantitative measure of *in vivo* chromosome damage (HEDDLE 1973). Micronuclei (MN) can arise from acentric chromosome fragments or whole chromosomes that have not been incorporated in the main nuclei at cell division (NUSSE *et al.* 1996). The formation of micronuclei can be stimulated by DNA-damaging agents that induce chromosome breaks or abnormal chromosome segregation, and thus the micronucleus assay has been used as a genetic toxicology tool for quantitative analysis of *in vivo* chromosome damage induced by potential mutagens (MORITA *et al.* 1997). A peripheral blood micronucleus assay has been semiautomated by flow cytometry (DERTINGER *et al.* 1996), making it practical for screening large numbers of mice with high statistical power. We show that this assay has the ability to detect spontaneous and radiation-induced chromosome instability in DSB repair-deficient homozygous *Atm* (ataxia telangiectasia-mutated) and *Prkdc*$^{scid}$ (severe combined immune deficiency) mutant mice.

Here we report a small-scale ENU mutagenesis screen for chromosome instability mutants that yielded three mutations and one potential mutation causing higher spontaneous micronucleus levels. One of the recovered mutations also confers higher radiation-induced micronucleus levels. This newly identified mutation was named *chaos1* (*ch*romosome *a*berration *o*ccurring *s*pontaneously *1*) and mapped to a 1.3-Mb region of chromosome 16 that does not contain any genes known to cause chromosome instability in humans or mice. However, we identified a mutation in *Polq*, an ortholog of Drosophila *mus308*, that resides in this region. Flies mutant at this locus exhibit genome instability and hypermutability in response to certain chemical agents (LEONHARDT *et al.* 1993). These experiments demonstrate the robustness of the flow cytometric micronucleus assay as a high-throughput screening tool to detect mutations causing genome instability and potential cancer susceptibility.

## MATERIALS AND METHODS

**ENU mutagenesis:** ENU preparation and the injection protocol was based on described protocols (JUSTICE 1999). Male C57BL6/J (B6) mice were intraperitoneally injected with 80 mg ENU/kg body weight (Sigma, St. Louis) once a week for 3 weeks at 8–10 weeks of age. They were mated to C3HeB/FeJ (C3H) females to obtain first generation ($G_1$) sons. The $G_1$ males were mated to C3H females to obtain second generation ($G_2$) daughters. In the whole-genome screens, up to four $G_2$ daughters were backcrossed to their $G_1$ fathers to generate third-generation ($G_3$) offspring who were potentially homozygous for mutations transmitted by the $G_1$. Micronucleus assays were performed on male $G_3$ progeny.

Some of the animals screened were derived from a region-specific mutagenesis program focused on the ~30-cM region on proximal chromosome 5 spanned by the rump white (*Rw*) inversion. Mutagenized B6 mice were crossed to C3H-*Rw*/+ females, and resulting $G_1$ males inheriting *Rw* (*Rw*/+*, where the asterisk represents the mutagenized chromosome 5) were crossed to *Rw/Hm* females (*Hm* refers to hammertoe, a semidominant mutation causing webbing of the digits) to yield *Rw*/+* $G_2$ offspring. Unlike the previous cross where $G_2$'s were crossed to the $G_1$ father, in this case the $G_2$'s were intercrossed to produce the $G_3$ generation. Since *Rw* contains a recessive lethal, only *Rw*/+* and +*/+* $G_3$ offspring were produced. Only 1 +*/+* $G_3$ male per family was screened by the micronucleus assay. Note that, as a result of the intercross of the $G_2$'s, the non-chromosome 5 mutations could be rendered homozygous, but the proportion of these compared to the former screen is half ($G_2$ animals carry half the mutational load of a $G_1$).

**Irradiation of mice and flow cytometric micronucleus assay:** Six-week-old $G_3$ males were exposed to 0.7 Gy of γ-rays from a $^{137}$Cs source. Forty-eight hours later, 50 μl of peripheral blood was collected from the retro-orbital sinus into a tube containing 250 μl of anticoagulant solution (500 USP heparin/ml saline, Sigma). A total of 180 μl was transferred to a polypropylene centrifuge tube containing 2 ml methanol at −80°. The tubes were struck sharply several times to break up aggregates and then stored at least overnight before further processing. Flow cytometric analysis was performed on a FACScan cytometer (Becton-Dickinson, San Jose, CA) as described (DERTINGER *et al.* 1996). At least 10,000 reticulocytes and 500,000 normochromatic erythrocytes were analyzed per blood sample.

**Microscopic scoring of micronuclei:** A method using acridine orange (Sigma)-coated slides (HAYASHI *et al.* 1990) was used to score micronuclei under a fluorescent microscope. Five thousand reticulocytes per sample were analyzed for the presence of micronuclei.

**SCID phenotyping:** A total of 100 μl peripheral blood in

anticoagulant solution was added to 1 ml fluorescence-activated cell sorter (FACS) buffer (Ca/Mg free PBS, 5 mM EDTA, 0.02% $NaN_3$), mixed, and set on ice. Four milliliters of Gey's buffer (HBSS, 650 mM $NH_4Cl$, 27 mM glucose) was added to the mixture and placed for 5 min on ice. Cells were pelleted at 500 × *g* for 5 min at 10°. The pellet was washed twice with 4 ml Gey's buffer and once with 4 ml FACS buffer and then resuspended. Fc receptors were blocked for 30 min on ice with a cocktail of anti-CD16/32 (FcγII/II Rc, produced in house) and Rat IgG (Sigma) using 10 μg of each per blood sample. They were then stained with 145-2C11 (hamster anti-mouse CD3ε) phycoerythrin (PE) to label any T-lymphocytes and with anti-mouse Ig κ, light chain FITC (PharMingen, San Diego) for B-lymphocytes. All antibodies were pretitrated for optimal concentration. Staining occurred on ice for 30 min, after which cells were washed with 2 ml FACS buffer, pelleted, and resuspended in 250 μl FACS buffer. A total of 10 μl propidium iodide solution (20 μg/ml in FACS buffer) was added prior to running samples on the FACScan for live/dead cell discrimination.

**Polymerase chain reaction (PCR) analysis of microsatellite markers:** Genomic DNA was prepared from the tails as described elsewhere (Truett *et al.* 2000). Three microliters of genomic DNA was amplified in a total reaction volume of 30 μl under standard PCR conditions. PCR products were analyzed on 3.75% MetaPhor gels (BMA, Rockland, ME).

**Reverse transcription-PCR analysis of *Polq* cDNA:** Total RNA was extracted from testes using the RNeasy midi kit (QIAGEN, Valencia, CA). Five micrograms of total RNA were used for RT reactions with Super-ScriptII (GIBCO BRL, Rockville, MD) followed by PCR using *Polq* primer pairs. The primer sequences are available upon request. Rapid amplification of cDNA ends (RACE) was conducted with the 5′ RACE system kit and 3′ RACE adapter primer (GIBCO BRL). cDNA was sequenced on an ABI 3700 DNA analyzer (Applied Biosystems, Foster City, CA).

## RESULTS

**High-throughput assay for detecting chromosome instability in mice:** Phenotype-driven mutagenesis is a powerful way to identify new genes and their biological roles in the context of a whole organism. In seeking a high-throughput assay suitable for identifying mutations causing elevated levels of chromosome damage *in vivo*, a highly sensitive and reproducible flow cytometric peripheral blood micronucleus assay (Dertinger *et al.* 1996) was evaluated.

In peripheral blood, micronuclei can be enumerated clearly in erythrocytes, which expel their nuclei, but not micronuclei, after their last mitotic division. To facilitate the formation of micronuclei, mice were exposed to 0.7 Gy γ-rays from a $^{137}Cs$ source. In a control experiment, blood was analyzed from a wild-type mouse before and 48 hr after irradiation. In erythrocytes, normochromatic erythrocytes (NCEs) and reticulocytes (RETs) can be distinguished with an anti-CD71 antibody (Serke and Huhn 1992), and micronuclei are stainable with the nucleic acid binding agent propidium iodide. The frequency of reticulocytes with micronuclei (MN-RETs) increased from 0.29 to 2.6% at 48 hr after γ-irradiation (Figure 1). Induced micronuclei would be observed in RETs, because micronucleus formation requires a mitosis and RETs in the peripheral blood are products of the most recent mitotic cycle. On the other hand, because NCEs lacked nuclei at the time of irradiation, the frequency of MN-NCEs remained relatively constant before and after irradiation; these micronuclei are of spontaneous origin. Therefore, both spontaneous and radiation-induced micronucleus levels could be measured simultaneously in the same sample.

The data obtained by flow cytometry were compared to those obtained by microscopic manual scoring of the same samples. A high correlation ($r^2 = 0.96$) was achieved, demonstrating that the flow cytometric scoring accurately reflects classical micronucleus scoring.

**Elevated incidence of micronuclei in DSB-repair-deficient mice:** To test the sensitivity and efficacy of the assay in detecting genomic instability/DSB repair mutants, we used two types of radiation-sensitive mice, 129S6/SvEvTac-*Atm*$^{tm1Awb}$ (*Atm*$^{-/-}$) and NOD.CB17-*prkdc*$^{scid}$/J (NOD scid). As shown in Figure 2, these mutants had significantly higher micronucleus frequencies at 48 hr after irradiation than did controls ($P < 0.0005$ for both *Atm*$^{-/-}$ and NOD scid using the two-tailed *t*-test). In contrast to the SCID mice, the percentage of MN-RETs in *Atm*$^{-/-}$ mice prior to irradiation was significantly higher ($P < 0.0001$) than that in controls, indicating that these mice have intrinsically elevated chromosome instability. These results demonstrate the potential usefulness of this assay as a screening tool for mutations causing both spontaneous and radiation-induced chromosome instability.

**Mutagenesis screen to isolate chromosome instability mutations:** To identify new mutations, we mutagenized male C57BL6/J (B6) mice with ENU and used them to initiate a three-generation breeding scheme to obtain third-generation ($G_3$) offspring that were potentially homozygous for induced mutations (see Materials and Methods). ENU is a potent germline point mutagen that produces functional mutations at a rate of ~1/750/locus/gamete (Hitotsumachi *et al.* 1985). $G_3$ males were screened by the micronucleus assay to detect recessive mutations affecting radiation-induced and/or spontaneous micronucleus frequencies.

In Figure 3, representative distributions of spontaneous and γ-ray-induced micronucleus frequencies in 127 $G_3$ males are plotted. The means (with standard deviation) were 0.21 ± 0.08% and 2.35 ± 0.70% for spontaneous and γ-ray-induced micronucleus frequencies, respectively (Figure 3, A and B).

Three different screens were conducted. In the first, 422 $G_3$ males descended from 39 $G_1$ males were tested for elevated spontaneous and radiation-induced micronucleus levels. One variant appeared as an outlier, which was defined as an individual with micronucleus levels higher than three standard deviations of the mean. This variant exhibited significantly elevated levels of both

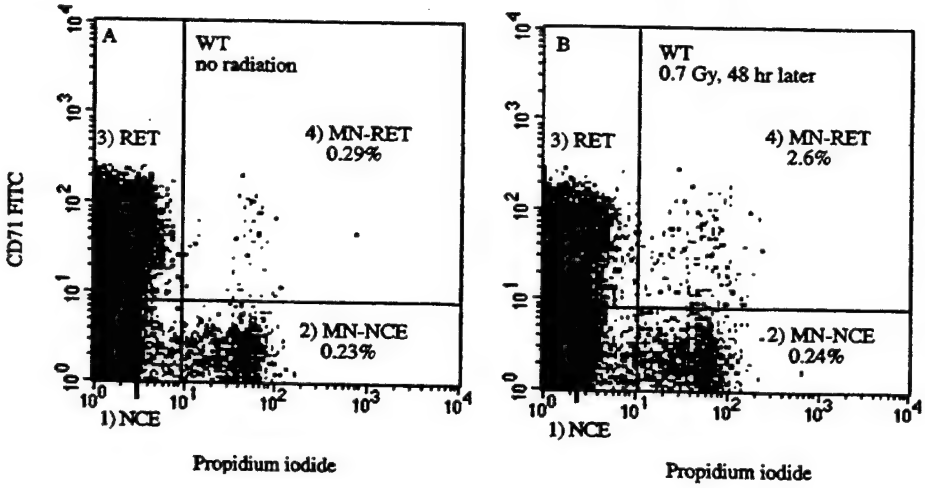


FIGURE 1.—Representative data from the flow cytometric micronucleus assay. Peripheral blood from a wild-type animal before (A) and 48 hr after (B) γ-irradiation was analyzed. CD71-positive RETs (populations 3 and 4) are separated from CD71-negative NCEs (populations 1 and 2) to enumerate radiation-induced micronuclei. MN-NCEs and MN-RETs are stained with propidium iodide and shown as populations 2 and 4, respectively.

spontaneous and radiation-induced micronucleated erythrocytes (Figure 3, A and B). Moreover, the number of RETs was decreased markedly after irradiation (to 0.26% of total erythrocytes) as seen in Figure 3C, indicating its hypersensitivity to γ-rays. This trait was determined to be recessive and exhibited Mendelian segregation. This mutation, *chaos1*, is described below.

Since a positive correlation between spontaneous and induced micronucleus levels has been reported in a number of mouse strains (SALAMONE and MAVOURNIN 1994), mice generated in the subsequent screens were tested only for spontaneous micronucleus levels. In the second screen, one potential mutation was recovered among 212 $G_3$ males derived from 20 $G_1$ males. This potential mutation is being tested to characterize radiation sensitivity and genetic heritability. The third screen involved mice produced in an ongoing region-specific mutagenesis project in our laboratory designed to detect various mutations on proximal chromosome 5 (SCHIMENTI and BUCAN 1998). Out of 336 $G_3$ males screened from 336 families (see MATERIALS AND METHODS), we have identified two mutations conferring higher spontaneous micronucleus levels. However, these two mutations were not linked to chromosome 5. Overall, three mutations and one potential mutation have been recovered among 970 $G_3$ males derived from 395 $G_1$ males. The results of all the screens are summarized in Table 1.

***chaos1* mutation:** Since the DNA content of micronuclei in *chaos1/chaos1* mice spans a wide range, it is likely that the micronuclei contain fragments of chromosomes, indicative of a failure to properly repair DSBs. DSBs are repaired in mammalian cells by one of two pathways: NHEJ and HR. Mice deficient in all known components of the NHEJ pathway show a SCID phenotype, due to defects in V(D)J recombination that lead to serious impairment of immune function (MULLER *et al.* 1999). Although there were no overt indications that *chaos1* mutants were immunodeficient, experiments were performed to test this possibility. Peripheral blood of *chaos1/chaos1* mice was stained with anti-CD3ε-PE and anti-Ig κ light chain-FITC antibodies to mark T- and B-cells, respectively. *chaos1/chaos1* mice had normal numbers of B- and T-cells, unlike a classic SCID profile (Figure 4A). To evaluate *chaos1* mutants for potential HR repair defects, we challenged them with mitomycin C (MMC), which causes DNA interstrand crosslinks. Since mutations in the *RAD51*-related genes *XRCC2* and *XRCC3* confer MMC hypersensitivity, it has been sug-

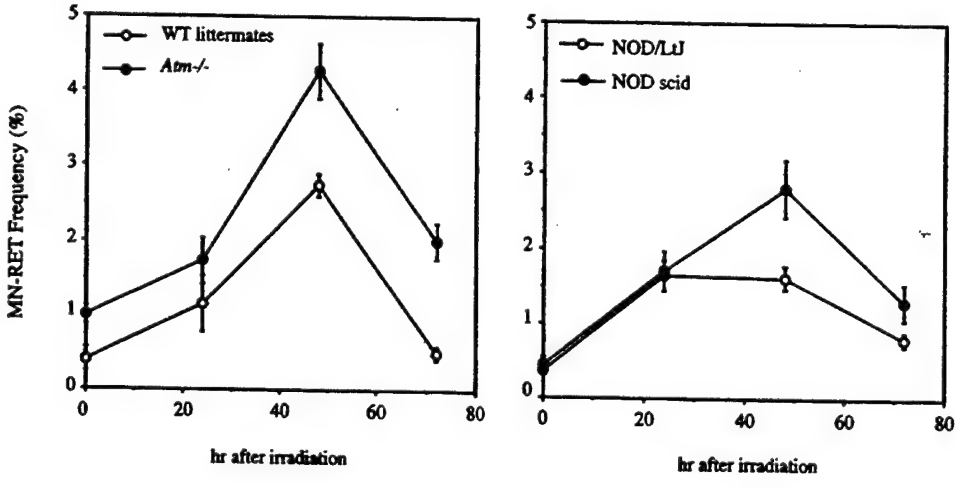


FIGURE 2.—Higher micronucleus levels in radiation-sensitive mutants. Homozygous mutants at *Atm* or *Prkdc* and their control strains (wild-type littermates for $Atm^{-/-}$ mutants and NOD/LtJ for NOD scid) were exposed to 0.7 Gy γ-ray. Peripheral blood was collected from the animals every 24 hr up to 72 hr from the time of irradiation and was analyzed by the flow cytometric micronucleus assay. Each point is shown with standard deviation. At least five animals were used per group.

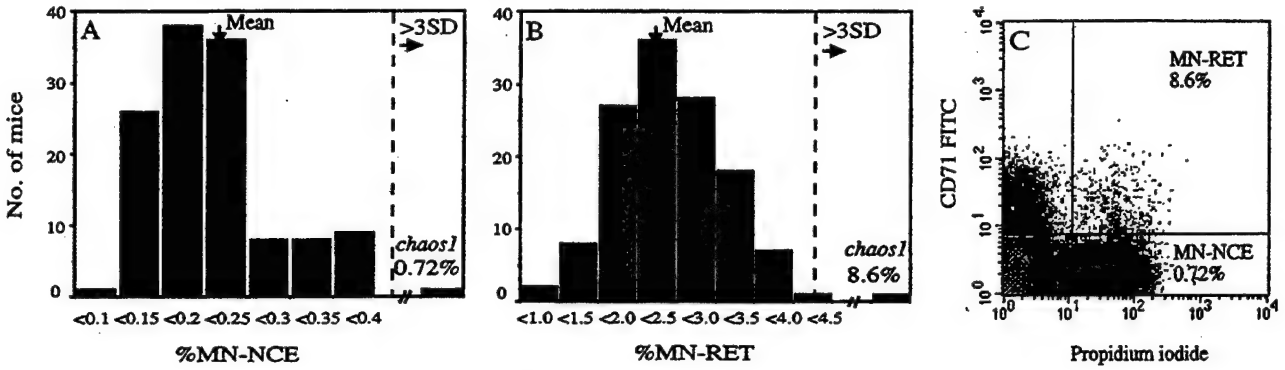


FIGURE 3.—Distribution of micronucleus frequency in NCEs and RETs in $G_3$ animals. *chaos1* appeared as an outlier with significantly higher spontaneous (A) and radiation-induced (B) micronucleus frequencies. Both exceed three standard deviations (3 SD). The flow plot of *chaos1* is shown in C. Two million erythrocytes were analyzed to collect 5000 RETs because of an extremely low number of RETs in this mutant after irradiation.

gested that crosslinks are repaired by the HR pathway (THACKER 1999). *chaos1/chaos1* mice had higher levels of micronuclei in response to MMC than did their wild-type littermates ($P = 0.0039$; see Figure 4B), suggesting that these mice are defective in HR repair or crosslink repair.

Aside from the phenotypes of elevated micronuclei and radiosensitivity of reticulocytes, *chaos1/chaos1* mutants are fertile and appear normal in all other respects up to 18 months of age. Radiation-induced tumorigenesis is being investigated in *chaos1/chaos1* mice rendered congenic in particular strain backgrounds. Tail fibroblasts isolated from *chaos1/chaos1* mice did not appear to be significantly sensitive to radiation compared to those from wild type (data not shown); thus this phenotype might be restricted to hematopoietic cells.

***chaos1* mapping:** We genetically mapped *chaos1* to an ~3-cM interval between *D16Mit4* and *D16Mit125* on chromosome 16 by performing genome scans of affected animals (97 meioses) produced in matings of homozygous $G_3$ animals to their heterozygous $G_1$ or $G_2$ parents (using microsatellite markers polymorphic between B6 and C3H). We then conducted a larger intersubspecific backcross by crossing *chaos1/chaos1* mice to *Mus castaneus* (CAST/Ei) and then backcrossing the $F_1$'s to *chaos1* homozygotes. The resulting 1710 progeny were typed with existing and newly developed polymorphic microsatellite markers in the critical region of MMU16, and recombinants were phenotyped by the micronucleus assay. Exploiting the mouse genomic sequences in the Celera Discovery System (CDS), we localized *chaos1* to a 1.3-Mb interval between *D16Mit11* and a new marker, *D16Jcs23* (Figure 5). Information on *chaos1* mapping has been deposited in the Mouse Genome Database (accession no. J:73427).

***Polq* as a candidate gene for *chaos1*:** The *chaos1* critical region is homologous to human chromosome 3q13.31, which contains the *POLQ* gene, encoding DNA polymerase θ (SHARIEF *et al.* 1999). Among 22 genes predicted by the CDS in the *chaos1* critical region (see Figure 5), *Polq* is an attractive candidate for *chaos1*, because its protein sequence is homologous to that encoded by *Drosophila melanogaster mus308* (*mu*tagen *s*ensitivity *308*), a gene believed to be involved in interstrand crosslink repair (BOYD *et al.* 1990). *mus308* encodes a 229-kD polypeptide containing seven conserved motifs characteristic of DNA and RNA helicases in an amino-terminal domain. The carboxy-terminal domain shares similarity

**TABLE 1**

**Summary of the MN screens**

| Type of screen | No. of $G_3$ males | No. of $G_1$ males | No. of mutations | Remarks |
|---|---|---|---|---|
| Genome wide | | | | |
| Radiation-induced and spontaneous MN | 422 | 39 | 1 | *chaos1* |
| Spontaneous MN | 212 | 20 | 1 | Putative |
| Chromosome 5 | | | | |
| Spontaneous MN | 336[a] | 336 | 2[b] | |
| Total | 970 | 395 | 4 | |

[a] $G_3$ animals in this screen were generated by intercrosses between $G_2$ males and $G_2$ females.
[b] These mutations are not linked to chromosome 5.

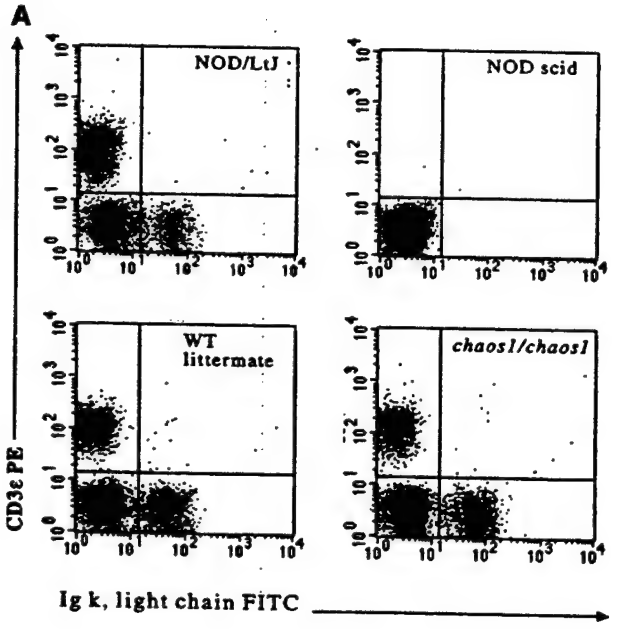


FIGURE 4.—Phenotypes of *chaos1/chaos1* mice. (A) *chaos1* mutants have normal B- and T-cell production. Peripheral blood from *chaos1/chaos1* mice and their wild-type littermate was stained with anti-Ig κ light chain and anti-CD3ε-PE to label B- and T-cells, respectively. NOD/LtJ and NOD scid mice were used as positive and negative controls, respectively. (B) Mitomycin C sensitivity of *chaos1* mutants revealed by the micronucleus assay. *chaos1* mutants and their wild-type littermates were given 1 mg/kg of MMC. Peripheral blood was sampled every 24 hr and analyzed for MMC-induced micronuclei in RETs. At least five animals were used per group and data are shown with standard deviations.

with the polymerase domain of prokaryotic DNA polymerase I-like enzymes (HARRIS *et al.* 1996). The presence of two such domains in a protein is unique.

The CDS predicted the existence of a gene sharing homology with human *POLQ* in the *chaos1* critical region. RT-PCR was performed with primers designed to the predicted mouse gene, yielding partial cDNAs from testis of B6 mice. The overlapping partial cDNAs were used to identify an open reading frame of 7635 nucleotides (Figure 6A), which encodes a polypeptide of 2544 amino acids (GenBank accession no. AY074936). As predicted, this polypeptide contains helicase and DNA polymerase motifs and it has 68% amino acid identity to human POLQ containing 2724 amino acids (AY032677; Clustal W 1.4 alignment).

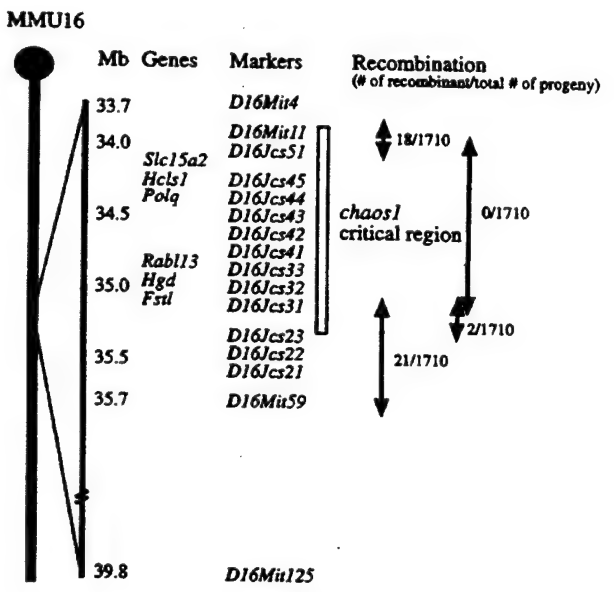


FIGURE 5.—The *chaos1* critical region. Physical location of all known genes and microsatellite markers are shown, using data from the Celera Discovery System. *D16Jcs* markers, which are polymorphic between B6 and CAST/Ei, were designed for this study. Data from the intersubspecific mapping backcross between *chaos1* and CAST/Ei, which were used to determine the *chaos1* critical region, are shown. Twenty-two genes predicted by the CDS are in this region.

The Celera mouse genome sequence was used to reveal that a total of 30 exons comprise this *Polq* cDNA (Figure 6A). Similarly, exploiting the Celera human genome sequence, 31 exons were found for *POLQ*. As shown in Figure 6B, a shorter transcript, which skips exons 6–10, was also found in mouse testis, giving rise to a predicted polypeptide of 2265 amino acids (AY147862). Moreover, each of the *Polq* transcripts has a longer isoform containing one extra exon (exon 4); however, the presence of this exon creates a stop codon (AY147863, AY147864). A Riken mouse cDNA from neonatal thymus has full-length exons 2 and 5, also containing a stop codon (AK020790). Collectively, 31 *Polq* exons were found; however, the roles of these various transcripts remain to be elucidated.

There was no indication of differences in transcript size or expression levels in mutant RNA compared to that from wild-type B6 mice (data not shown). Nevertheless, a single T → C base substitution was identified at residue 5794 in the coding region (exon 19) of the *chaos1*

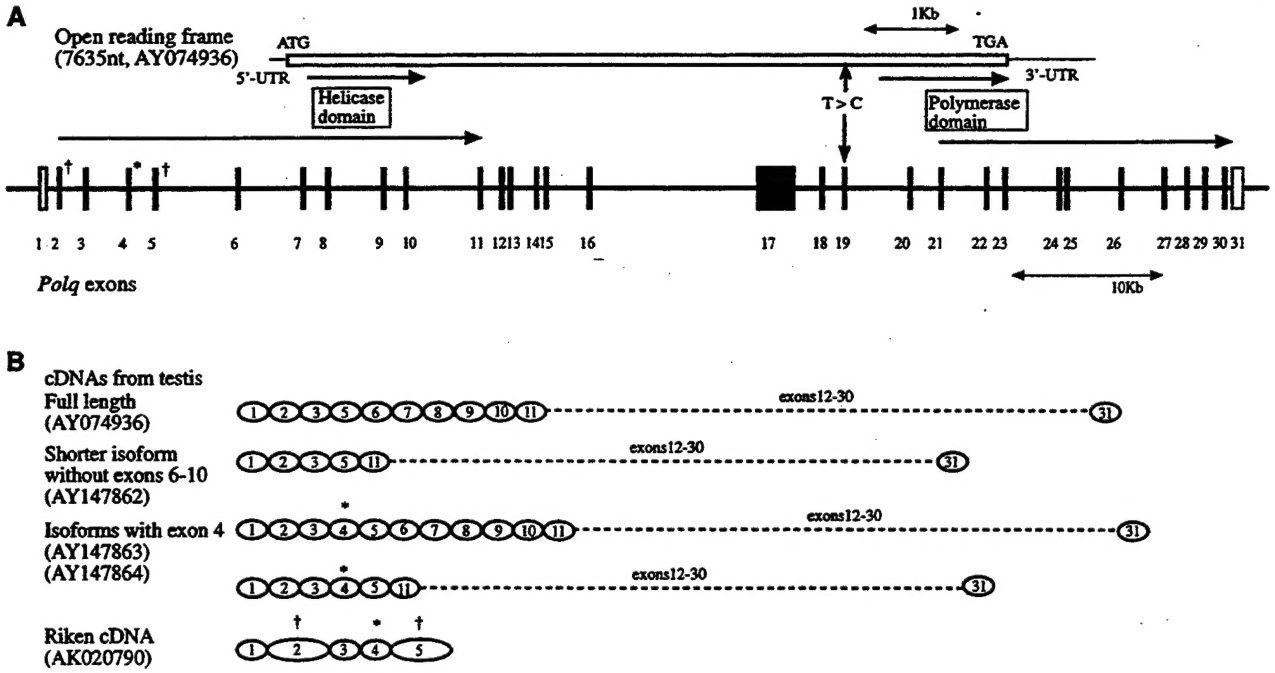


FIGURE 6.—Structure of the *Polq* gene and transcripts. (A) An open reading frame flanked by 5′- and 3′-untranslated regions (UTR) in *Polq* cDNA is shown to scale (above) with the start codon and stop codon. The Celera mouse genome sequence was used to reveal that a total of 30 exons encode this *Polq* cDNA (AY074936). Exons (small rectangles) and introns in the *Polq* gene are shown to scale (below). Exons 1 and 31 (small unfilled rectangles) contain the 5′- and 3′-UTRs, respectively. The T → C transition found in *chaos1* mutant is indicated. The regions of helicase and DNA polymerase homology and the corresponding exons are also indicated as arrows. (B) Schematic illustration of exons comprising the different *Polq* transcripts. A shorter transcript that skips exons 6–10 was also identified (AY147862). (*) Longer isoforms containing one extra exon (exon 4) were also identified; however, the presence of this exon creates a stop codon (AY147863, AY147864). (†) Full-length exons 2 and 5 were found in a Riken mouse cDNA from neonatal thymus (AK020790), whereas *Polq* cDNAs from testis contain only part of exons 2 and 5, because of alternative splicing of these exons. Collectively, 31 *Polq* exons were found.

mutant allele (Figure 6A), which is not present in B6 cDNA. This mutation gives rise to a serine-to-proline change at residue 1932.

## DISCUSSION

To our knowledge, this is the first successful phenotype-driven screen for chromosome instability mutants in mice. The micronucleus assay adapted from the method developed by DERTINGER *et al.* (1996) was highly sensitive and readily implemented as a high-throughput screen for mutagenized mice. The dose of γ-rays used in this screen had little effect on the reproductive ability of the $G_3$ males, which were subsequently used for mapping studies or maintenance of the mutation. Only males were screened in this study due to logistical factors associated with the mutagenesis program from which the mice were derived. However, the spontaneous micronucleus frequencies tended to be lower in females than in males.

Importantly, the high reproducibility of the assay (DERTINGER *et al.* 2000; TOROUS *et al.* 2001) allowed accurate phenotyping of mice in the mapping crosses, which is critical for positional cloning. In the case of *chaos1* phenotyping, there was no need to irradiate mice, because the mutants were easily identified by high spontaneous micronucleus levels. Actually, we find it more practical and feasible to perform screens only for spontaneously elevated micronucleus levels. Potential mutants isolated can be characterized later as to sensitivity to radiation or other agents. Moreover, micronuclei can be isolated by flow sorting or microdissection for further analysis (NUSSE *et al.* 1996; PEACE *et al.* 1999) to characterize phenotypes of identified mutants.

The presence of a mutated *Polq* allele in *chaos1* mice makes this gene a strong candidate for *chaos1*. The identified T → C transition is one of the two most frequent classes of ENU-induced mutations in the mouse germline (MARKER *et al.* 1997; JUSTICE *et al.* 1999). This mutation causes a drastic amino acid change in POLQ from serine to proline, which may alter the secondary structure of the molecule. However, since the mutation is not located in either the helicase or the polymerase domains of the predicted protein (the two regions of the protein about which we can make informed speculation as to key enzymatic activity), it is difficult to draw a conclusion about the functional importance of this

particular amino acid residue or to determine if the mutation actually compromises protein function. To gain some insight into the functional importance of this amino acid residue, we compared the mouse POLQ sequence to those of other organisms. Homologs of *mus308* have been reported in *Caenorhabditis elegans*, *Arabidopsis thaliana* (Harris *et al.* 1996; Marini and Wood 2002), and humans (Sharief *et al.* 1999), but not yeast. By BLAST searching databases, we also found a presumed ortholog in *Anopheles gambiae* (mosquitos; accession no. EAA04696). The serine is conserved in human and mosquito. It exists as alanine in Drosophila (L76559) and asparagine in Arabidopsis (CAA18591), both of which are semiconservative differences. The region containing this residue in *C. elegans* (AAB93325) is too divergent to align with other *mus308* homologs.

Additional support for *Polq* as a candidate for *chaos1* is the similarity in phenotypes of *chaos1* mutants to flies containing mutations in *mus308*, a *Polq* homolog. Drosophila *mus308* encodes a unique protein with helicase and prokaryotic DNA polymerase I-like motifs in a single polypeptide (Harris *et al.* 1996). *mus308* mutants were identified as strains hypersensitive to nitrogen mustard, a crosslinking agent (Boyd *et al.* 1981), but not to a monofunctional alkylating agent, methyl methanesulfonate (Boyd *et al.* 1990), suggesting that *mus308* is specifically involved in crosslink repair. However, it has been reported that *mus308* might be also involved in postreplicational repair (Aguirrezabalaga *et al.* 1995; Tosal *et al.* 2000). Homozygous *mus308* flies showed elevated embryonic mortality associated with chromosome instability and a mutator phenotype in response to certain mutagens (Leonhardt *et al.* 1993).

Recently, human POLQ was purified as a high-fidelity DNA polymerase with the ability to bypass DNA lesions (Maga *et al.* 2002). This is quite unique among recently discovered DNA polymerases, most of which are error prone (Goodman and Tippin 2000). However, the purified POLQ did not show detectable helicase activity (Maga *et al.* 2002). New helicase genes, *HEL308* and *Hel308*, which are homologous to the helicase motif of *mus308*, have been identified in humans and mice (Marini and Wood 2002). Purified human HEL308 exhibited a DNA helicase activity (Marini and Wood 2002). The existence of these paralogs may reflect redundancy in mammalian crosslink repair in which at least two pathways have been found: recombination-dependent and recombination-independent error-prone pathways (McHugh *et al.* 2001; Wang *et al.* 2001). It remains to be elucidated how exactly these proteins function to repair crosslinks. If *chaos1* is truly a *Polq* mutation, the *chaos1* mutant may fill a unique niche that would allow *in vivo* investigation of crosslink repair in mammals.

Despite the higher micronucleus levels, *chaos1/chaos1* mutants showed no apparent abnormalities up to 18 months of age. This may not be surprising, since mouse models for Fanconi anemia, which have defects in crosslink repair, do not show a predisposition to cancer (Chen *et al.* 1996; Cheng *et al.* 2000; Yang *et al.* 2001). It has also been reported that *Xpa* or *Xpc* knockouts, deficient in nucleotide excision repair, rarely developed tumors without carcinogen treatment (Wijnhoven *et al.* 2000; van Kreijl *et al.* 2001), although $Xpc^{-/-}$ mice had a higher spontaneous mutation rate at the *Hprt* locus. In general, genome instability itself may not be sufficient to cause cancer. Other events, such as loss of cell-cycle checkpoints, could be more critical. Nevertheless, chromosome instability may facilitate the occurrence of these critical events. Indeed, introduction of a *Trp53* null allele significantly enhanced mammary tumor formation in the *Brca1* conditional mutant mice; otherwise tumorigenesis occurred after long latency and at a low frequency (Xu *et al.* 1999; Deng and Scott 2000). We have also observed a synergistic increase in genome instability and growth retardation in mice doubly mutant for *Atm* and *chaos1* (N. Shima and J. Schimenti, unpublished data).

The data presented here demonstrate the efficacy of the micronucleus screen for detecting new chromosome instability mutants and subsequently mapping them in a robust way. With this screen, it is also possible that hypomorphic alleles of important DSB repair genes such as *Rad51* paralogs, whose complete inactivation causes embryonic lethality, may be detected (Thompson and Schild 1999). The genes responsible for elevated micronuclei might be involved not only in DNA repair, but also in processes such as mitotic-spindle checkpoints, defects of which could lead to aneuploidy, the most frequent genetic abnormality observed in cancer cells (Lengauer *et al.* 1998). While it is still controversial that genome instability always leads to carcinogenesis (Marx 2002), elevated micronucleus levels could be used as a surrogate phenotype that predicts cancer predisposition at an early age. In some cases, higher micronucleus levels in peripheral blood of humans have been linked with increased cancer risk (Doneda *et al.* 1995; Scott *et al.* 1999). Development of such a surrogate phenotype would enable the screening and mapping of recessive mutations causing cancers without aging mice to the point where late-onset cancers develop.

In conclusion, the flow cytometric screen for elevated micronuclei has proven to be a useful approach to identifying mutations in novel genes that cause genome instability as a consequence of DSB repair defects. The incorporation of these screens into major mutagenesis efforts may yield new and hitherto unknown genes that contribute to cancer and concomitantly may yield the cognate mutant mouse models.

We thank Leonard Shultz, Susan Ackerman, and Jeremy Ward for critical reading of the manuscript and helpful comments. This work is supported by National Institutes of Health grants GM-45415 and HD-35984 to J.S. N.S. is supported by a postdoctoral fellowship from the Breast Cancer Research Program, Department of Defense (DAMD 17-01-1-0277).

## LITERATURE CITED


AGUIRREZABALAGA, I., L. M. SIERRA and M. A. COMENDADOR, 1995 The hypermutability conferred by the mus308 mutation of Drosophila is not specific for cross-linking agents. Mutat. Res. **336:** 243–250.

BOYD, J. B., M. D. GOLINO, K. E. SHAW, C. J. OSGOOD and M. M. GREEN, 1981 Third-chromosome mutagen-sensitive mutants of *Drosophila melanogaster.* Genetics **97:** 607–623.

BOYD, J. B., K. SAKAGUCHI and P. V. HARRIS, 1990 mus308 mutants of Drosophila exhibit hypersensitivity to DNA cross-linking agents and are defective in a deoxyribonuclease. Genetics **125:** 813–819.

CHEN, M., D. J. TOMKINS, W. AUERBACH, C. MCKERLIE, H. YOUSSOUFIAN *et al.*, 1996 Inactivation of Fac in mice produces inducible chromosomal instability and reduced fertility reminiscent of Fanconi anaemia. Nat. Genet. **12:** 448–451.

CHENG, N. C., H. J. VAN DE VRUGT, M. A. VAN DER VALK, A. B. OOSTRA, P. KRIMPENFORT *et al.*, 2000 Mice with a targeted disruption of the Fanconi anemia homolog Fanca. Hum. Mol. Genet. **9:** 1805–1811.

DENG, C. X., and F. SCOTT, 2000 Role of the tumor suppressor gene Brca1 in genetic stability and mammary gland tumor formation. Oncogene **19:** 1059–1064.

DERTINGER, S. D., D. K. TOROUS and K. R. TOMETSKO, 1996 Simple and reliable enumeration of micronucleated reticulocytes with a single-laser flow cytometer. Mutat. Res. **371:** 283–292.

DERTINGER, S. D., D. K. TOROUS, N. E. HALL, C. R. TOMETSKO and T. A. GASIEWICZ, 2000 Malaria-infected erythrocytes serve as biological standards to ensure reliable and consistent scoring of micronucleated erythrocytes by flow cytometry. Mutat. Res. **464:** 195–200.

DIGWEED, M., A. REIS and K. SPERLING, 1999 Nijmegen breakage syndrome: consequences of defective DNA double strand break repair. Bioessays **21:** 649–656.

DONEDA, L., G. BASILISCO, P. BIANCHI and L. LARIZZA, 1995 High spontaneous chromosomal damage in lymphocytes from patients with hereditary megaduodenum. Mutat. Res. **348:** 33–36.

FRIEDBERG, E. C., G. C. WALKER and W. SIEDE, 1995 *DNA Repair and Mutagenesis.* ASM Press, Washington, DC.

GOODMAN, M. F., and B. TIPPIN, 2000 The expanding polymerase universe. Nat. Rev. Mol. Cell Biol. **1:** 101–109.

HARRIS, P. V., O. M. MAZINA, E. A. LEONHARDT, R. B. CASE, J. B. BOYD *et al.*, 1996 Molecular cloning of Drosophila mus308, a gene involved in DNA cross-link repair with homology to prokaryotic DNA polymerase I genes. Mol. Cell. Biol. **16:** 5764–5771.

HAYASHI, M., T. MORITA, Y. KODAMA, T. SOFUNI and M. ISHIDATE, JR., 1990 The micronucleus assay with mouse peripheral blood reticulocytes using acridine orange-coated slides. Mutat. Res. **245:** 245–249.

HEDDLE, J. A., 1973 A rapid in vivo test for chromosomal damage. Mutat. Res. **18:** 187–190.

HENDRICKSON, E. A., 1997 Cell-cycle regulation of mammalian DNA double-strand-break repair. Am. J. Hum. Genet. **61:** 795–800.

HITOTSUMACHI, S., D. A. CARPENTER and W. L. RUSSELL, 1985 Dose-repetition increases the mutagenic effectiveness of N-ethyl-N-nitrosourea in mouse spermatogonia. Proc. Natl. Acad. Sci. USA **82:** 6619–6621.

HRABE DE ANGELIS, M. H., H. FLASWINKEL, H. FUCHS, B. RATHKOLB, D. SOEWARTO *et al.*, 2000 Genome-wide, large-scale production of mutant mice by ENU mutagenesis. Nat. Genet. **25:** 444–447.

JONES, N. J., R. COX and J. THACKER, 1987 Isolation and cross-sensitivity of X-ray-sensitive mutants of V79-4 hamster cells. Mutat. Res. **183:** 279–286.

JONES, N. J., R. COX and J. THACKER, 1988 Six complementation groups for ionising-radiation sensitivity in Chinese hamster cells. Mutat. Res. **193:** 139–144.

JUSTICE, M. J., 1999 Mutagenesis of the mouse germline, pp. 185–215 in *Mouse Genetics and Transgenics: A Practical Approach,* edited by I. JACKSON and C. ABBOTT. Oxford University Press, Oxford.

JUSTICE, M. J., J. K. NOVEROSKE, J. S. WEBER, B. ZHENG and A. BRADLEY, 1999 Mouse ENU mutagenesis. Hum. Mol. Genet. **8:** 1955–1963.

KARRAN, P., 2000 DNA double strand break repair in mammalian cells. Curr. Opin. Genet. Dev. **10:** 144–150.

KHANNA, K. K., and S. P. JACKSON, 2001 DNA double-strand breaks: signaling, repair and the cancer connection. Nat. Genet. **27:** 247–254.

KRAAKMAN-VAN DER ZWET, M., W. J. OVERKAMP, R. E. VAN LANGE, J. ESSERS, A. VAN DUIJN-GOEDHART *et al.*, 2002 Brca2 (XRCC11) deficiency results in radioresistant DNA synthesis and a higher frequency of spontaneous deletions. Mol. Cell. Biol. **22:** 669–679.

LENGAUER, C., K. W. KINZLER and B. VOGELSTEIN, 1998 Genetic instabilities in human cancers. Nature **396:** 643–649.

LEONHARDT, E. A., D. S. HENDERSON, J. E. RINEHART and J. B. BOYD, 1993 Characterization of the mus308 gene in *Drosophila melanogaster.* Genetics **133:** 87–96.

MAGA, G., I. SHEVELEV, K. RAMADAN, S. SPADARI and U. HUBSCHER, 2002 DNA polymerase theta purified from human cells is a high-fidelity enzyme. J. Mol. Biol. **319:** 359–369.

MARINI, F., and R. D. WOOD, 2002 A human DNA helicase homologous to the DNA cross-link sensitivity protein Mus308. J. Biol. Chem. **277:** 8716–8723.

MARKER, P. C., K. SEUNG, A. E. BLAND, L. B. RUSSELL and D. M. KINGSLEY, 1997 Spectrum of *Bmp5* mutations from germline mutagenesis experiments in mice. Genetics **145:** 435–443.

MARX, J., 2002 Debate surges over the origins of genomic defects in cancer. Science **297:** 544–546.

MCHUGH, P. J., V. J. SPANSWICK and J. A. HARTLEY, 2001 Repair of DNA interstrand crosslinks: molecular mechanisms and clinical relevance. Lancet Oncol. **2:** 483–490.

MEYN, M. S., 1999 Ataxia-telangiectasia, cancer and the pathobiology of the ATM gene. Clin. Genet. **55:** 289–304.

MORITA, T., N. ASANO, T. AWOGI, Y. F. SASAKI, S. SATO *et al.*, 1997 Evaluation of the rodent micronucleus assay in the screening of IARC carcinogens (groups 1, 2A and 2B): the summary report of the 6th collaborative study by CSGMT/JEMS MMS. Collaborative Study of the Micronucleus Group Test. Mammalian Mutagenicity Study Group. Mutat. Res. **389:** 3–122.

MULLER, C., P. CALSOU, P. FRIT and B. SALLES, 1999 Regulation of the DNA-dependent protein kinase (DNA-PK) activity in eukaryotic cells. Biochimie **81:** 117–125.

NUSSE, M., B. M. MILLER, S. VIAGGI and J. GRAWE, 1996 Analysis of the DNA content distribution of micronuclei using flow sorting and fluorescent in situ hybridization with a centromeric DNA probe. Mutagenesis **11:** 405–413.

PEACE, B. E., G. LIVINGSTON, E. B. SILBERSTEIN and J. C. LOPER, 1999 A case of elevated spontaneous micronucleus frequency derived from chromosome 2. Mutat. Res. **430:** 109–119.

SALAMONE, M. F., and K. H. MAVOURNIN, 1994 Bone marrow micronucleus assay: a review of the mouse stocks used and their published mean spontaneous micronucleus frequencies. Environ. Mol. Mutagen. **23:** 239–273.

SCHIMENTI, J., and M. BUCAN, 1998 Functional genomics in the mouse: phenotype-based mutagenesis screens. Genome Res. **8:** 698–710.

SCOTT, D., J. B. BARBER, A. R. SPREADBOROUGH, W. BURRILL and S. A. ROBERTS, 1999 Increased chromosomal radiosensitivity in breast cancer patients: a comparison of two assays. Int. J. Radiat. Biol. **75:** 1–10.

SERKE, S., and D. HUHN, 1992 Identification of CD71 (transferrin receptor) expressing erythrocytes by multiparameter-flow-cytometry (MP-FCM): correlation to the quantitation of reticulocytes as determined by conventional microscopy and by MP-FCM using a RNA-staining dye. Br. J. Haematol. **81:** 432–439.

SHARIEF, F. S., P. J. VOJTA, P. A. ROPP and W. C. COPELAND, 1999 Cloning and chromosomal mapping of the human DNA polymerase theta (POLQ), the eighth human DNA polymerase. Genomics **59:** 90–96.

SHEN, S. X., Z. WEAVER, X. XU, C. LI, M. WEINSTEIN *et al.*, 1998 A targeted disruption of the murine Brca1 gene causes gamma-irradiation hypersensitivity and genetic instability. Oncogene **17:** 3115–3124.

THACKER, J., 1999 The role of homologous recombination processes in the repair of severe forms of DNA damage in mammalian cells. Biochimie **81:** 77–85.

THOMPSON, L. H., and D. SCHILD, 1999 The contribution of homologous recombination in preserving genome integrity in mammalian cells. Biochimie **81:** 87–105.

THOMPSON, L. H., and D. SCHILD, 2001 Homologous recombina-

tional repair of DNA ensures mammalian chromosome stability. Mutat. Res. **477:** 131–153.

THOMPSON, L. H., K. W. BROOKMAN, L. E. DILLEHAY, A. V. CARRANO, J. A. MAZRIMAS *et al.*, 1982 A CHO-cell strain having hypersensitivity to mutagens, a defect in DNA strand-break repair, and an extraordinary baseline frequency of sister-chromatid exchange. Mutat. Res. **95:** 427–440.

TOROUS, D. K., N. E. HALL, S. D. DERTINGER, M. S. DIEHL, A. H. ILLI-LOVE *et al.*, 2001 Flow cytometric enumeration of micronucleated reticulocytes: high transferability among 14 laboratories. Environ. Mol. Mutagen. **38:** 59–68.

TOSAL, L., M. A. COMENDADOR and L. M. SIERRA, 2000 The mus308 locus of Drosophila melanogaster is implicated in the bypass of ENU-induced O-alkylpyrimidine adducts. Mol. Gen. Genet. **263:** 144–151.

TRUETT, G. E., P. HEEGER, R. L. MYNATT, A. A. TRUETT, J. A. WALKER *et al.*, 2000 Preparation of PCR-quality mouse genomic DNA with hot sodium hydroxide and tris (HotSHOT). Biotechniques **29:** 52–54.

TUTT, A., A. GABRIEL, D. BERTWISTLE, F. CONNOR, H. PATERSON *et al.*, 1999 Absence of Brca2 causes genome instability by chromosome breakage and loss associated with centrosome amplification. Curr. Biol. **9:** 1107–1110.

VAN BRABANT, A. J., R. STAN and N. A. ELLIS, 2000 DNA helicases, genomic instability, and human genetic disease. Annu. Rev. Genomics Hum. Genet. **1:** 409–459.

VAN GENT, D. C., J. H. HOEIJMAKERS and R. KANAAR, 2001 Chromosomal stability and the DNA double-stranded break connection. Nat. Rev. Genet. **2:** 196–206.

VAN KREIJL, C. F., P. A. MCANULTY, R. B. BEEMS, A. VYNCKIER, H. VAN STEEG *et al.*, 2001 Xpa and Xpa/p53+/− knockout mice: overview of available data. Toxicol. Pathol. **29:** 117–127.

VENKITARAMAN, A. R., 2002 Cancer susceptibility and the functions of BRCA1 and BRCA2. Cell **108:** 171–182.

WANG, X., C. A. PETERSON, H. ZHENG, R. S. NAIRN, R. J. LEGERSKI *et al.*, 2001 Involvement of nucleotide excision repair in a recombination-independent and error-prone pathway of DNA interstrand cross-link repair. Mol. Cell. Biol. **21:** 713–720.

WIJNHOVEN, S. W., H. J. KOOL, L. H. MULLENDERS, A. A. VAN ZEELAND, E. C. FRIEDBERG *et al.*, 2000 Age-dependent spontaneous mutagenesis in Xpc mice defective in nucleotide excision repair. Oncogene **19:** 5034–5037.

XU, X., K. U. WAGNER, D. LARSON, Z. WEAVER, C. LI *et al.*, 1999 Conditional mutation of Brca1 in mammary epithelial cells results in blunted ductal morphogenesis and tumour formation. Nat. Genet. **22:** 37–43.

YANG, Y., Y. KUANG, R. M. DE OCA, T. HAYS, L. MOREAU *et al.*, 2001 Targeted disruption of the murine Fanconi anemia gene, Fancg/Xrcc9. Blood **98:** 3435–3440.

ZDZIENICKA, M. Z., 1999 Mammalian X-ray-sensitive mutants which are defective in non-homologous (illegitimate) DNA double-strand break repair. Biochimie **81:** 107–116.

Communicating editor: D. KINGSLEY